Higgs boson property measurements at the ATLAS experiment

Chara Kitsaki, on behalf of the ATLAS Collaboration
National Technical Univ. of Athens

DISCRETE2022: 8th Symposium on Prospects in the Physics of Discrete Symmetries
7-11 November 2022
Baden-Baden, Germany

The research work was supported by the Hellenic Foundation for Research and Innovation (HFRI) under the HFRI PhD Fellowship grant (Fellowship Number: 800)

Introduction

After the Higgs boson discovery by ATLAS and CMS in 2012

- statistically significant excess of events / properties consistent with SM prediction

the emphasis is shifted to the precise measurements of this new particle's properties
(i.e. mass, spin, parity, couplings, cross sections…)

- either put constraints or use it as gateway to physics BSM

The increase in the centre-of-mass energy to 13 TeV and the large dataset allowed further channels to be probed and precise measurements to be performed

Latest prediction from LHC Higgs Working Group

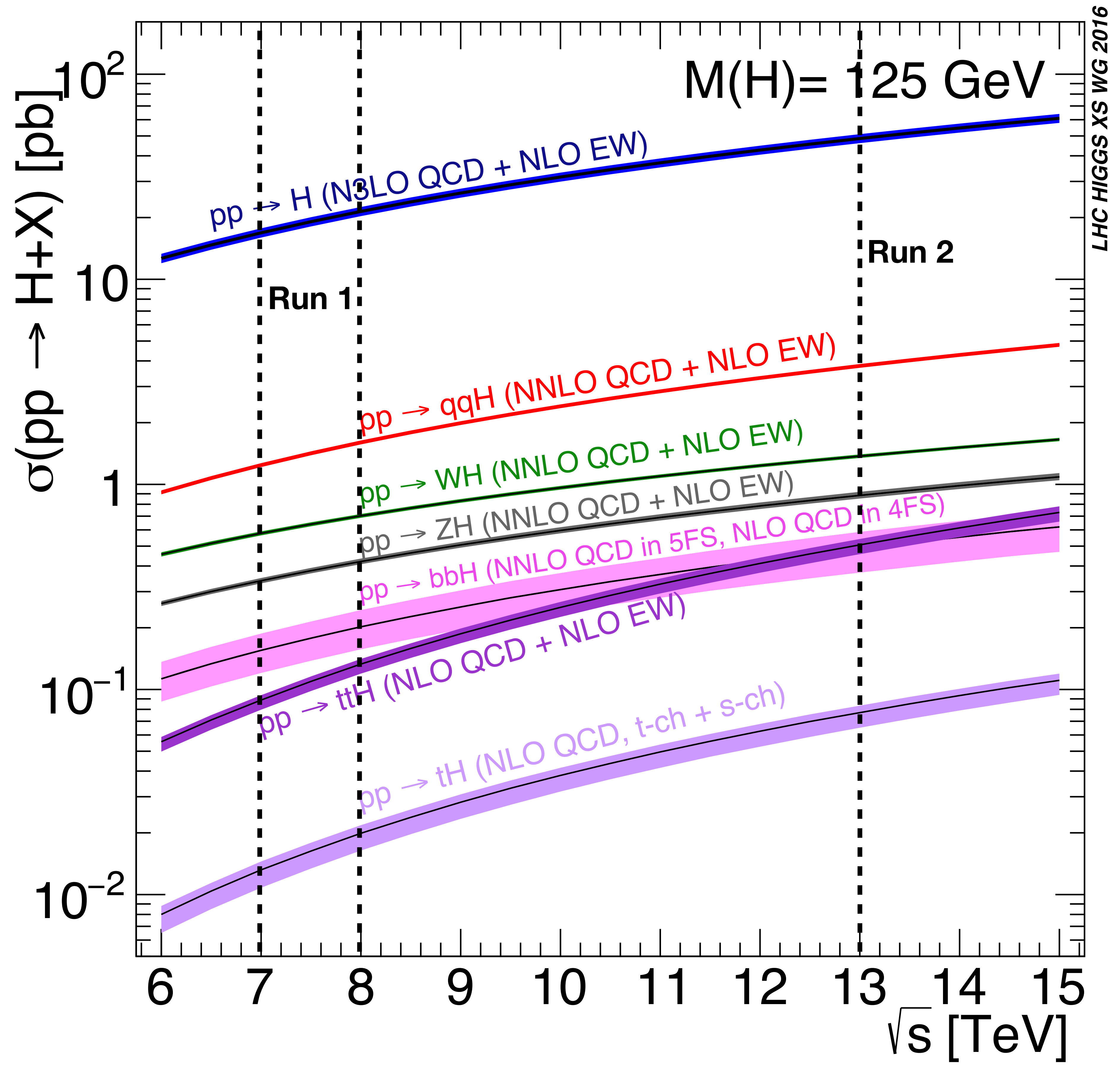

<u>This talk will highlight some of the most recent results for the Higgs boson by ATLAS</u>

Mass measurement

arXiv:2207.00320v1

$\mathrm{H} \rightarrow \mathrm{ZZ}^* \rightarrow 4\ell(=\mathrm{e} \text{ or } \mu)$

Improvements

more statistics

high-precision p_{T}^{μ} calibration

NN for S/B discrimination

event-level $m_{4\ell}$ resolution in the fit

Compatibility between channels: p-value of 0.82

ATLAS Run 1: $\sqrt{s} = 7-8$ TeV, 25 fb^{-1}

$m_H = 124.51 \pm 0.52$ GeV

ATLAS partial Run 2 (2015-2016): $\sqrt{s} = 13$ TeV, 36.1 fb^{-1}

$m_{\mathrm{H}} = 124.79 \pm 0.37$ GeV Phys. Lett. B 784 (2018) 345

ATLAS Full Run 2 (2015-2018): $\sqrt{s} = 13$ TeV, 139 fb^{-1}

$m_{\mathrm{H}} = 124.99 \pm 0.19$ GeV

Full Run 2

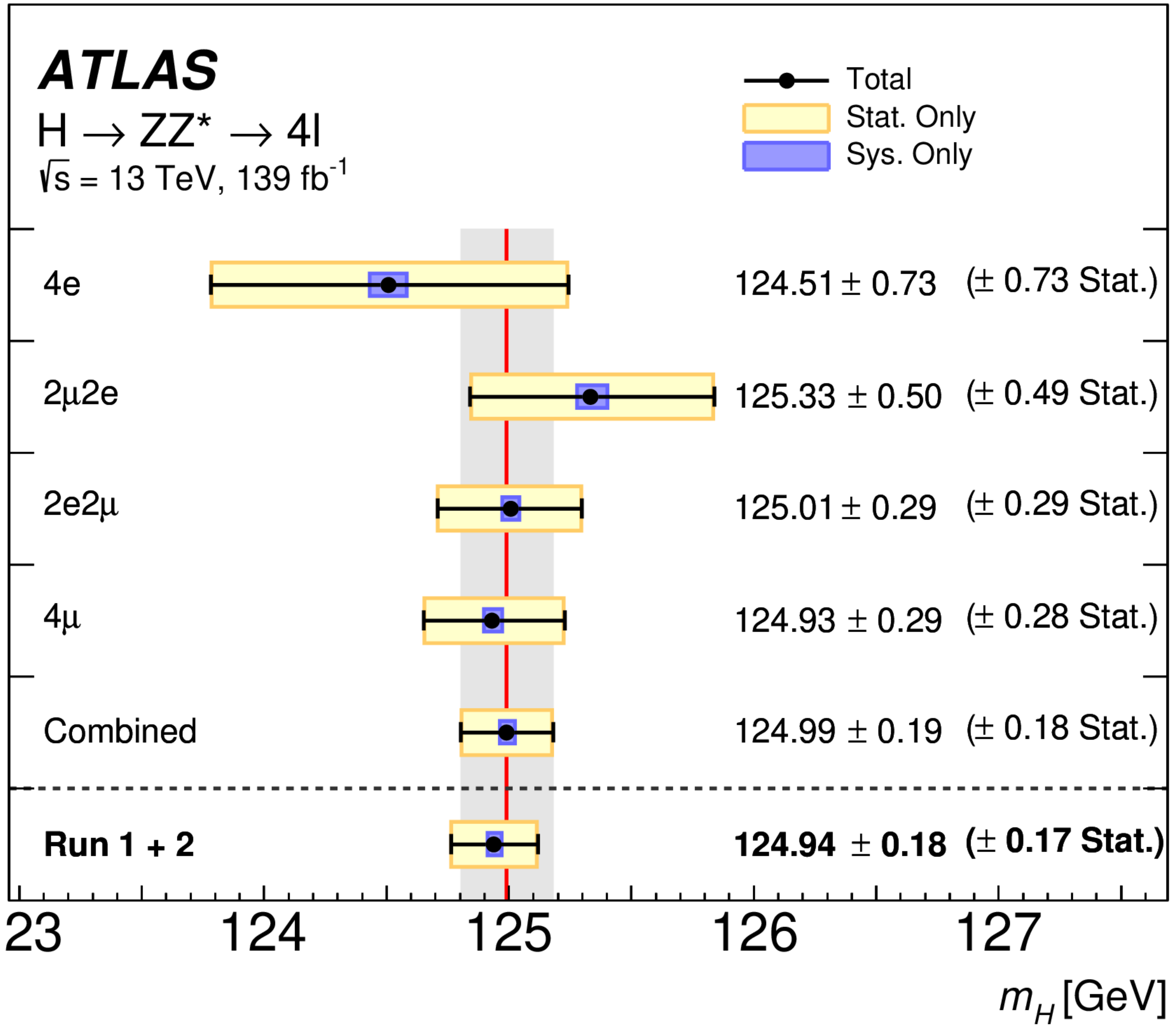

CP measurement

SM predicts a Higgs boson with spin 0 and positive parity ($J^{CP} = 0^{++}$)

with Run 1 dataset spin 1 and 2 hypotheses excluded with >99.9%CL

bosonic coupling in VBF $H \to \gamma\gamma$ channel arXiv:2208.02338v1

CP-odd component described by dim-6 EFT operators in HISZ and Warsaw bases:

Total Matrix element: $|\mathcal{M}|^2 = |\mathcal{M}_{SM}|^2 + 2 \cdot c_i \cdot \mathrm{Re}(\mathcal{M}^*_{SM}\mathcal{M}_{CP-odd}) + c_i^2 \cdot |\mathcal{M}_{CP-odd}|^2$ c_i: Wilson coefficient

Optimal Observable method: construct CP-sensitive observable

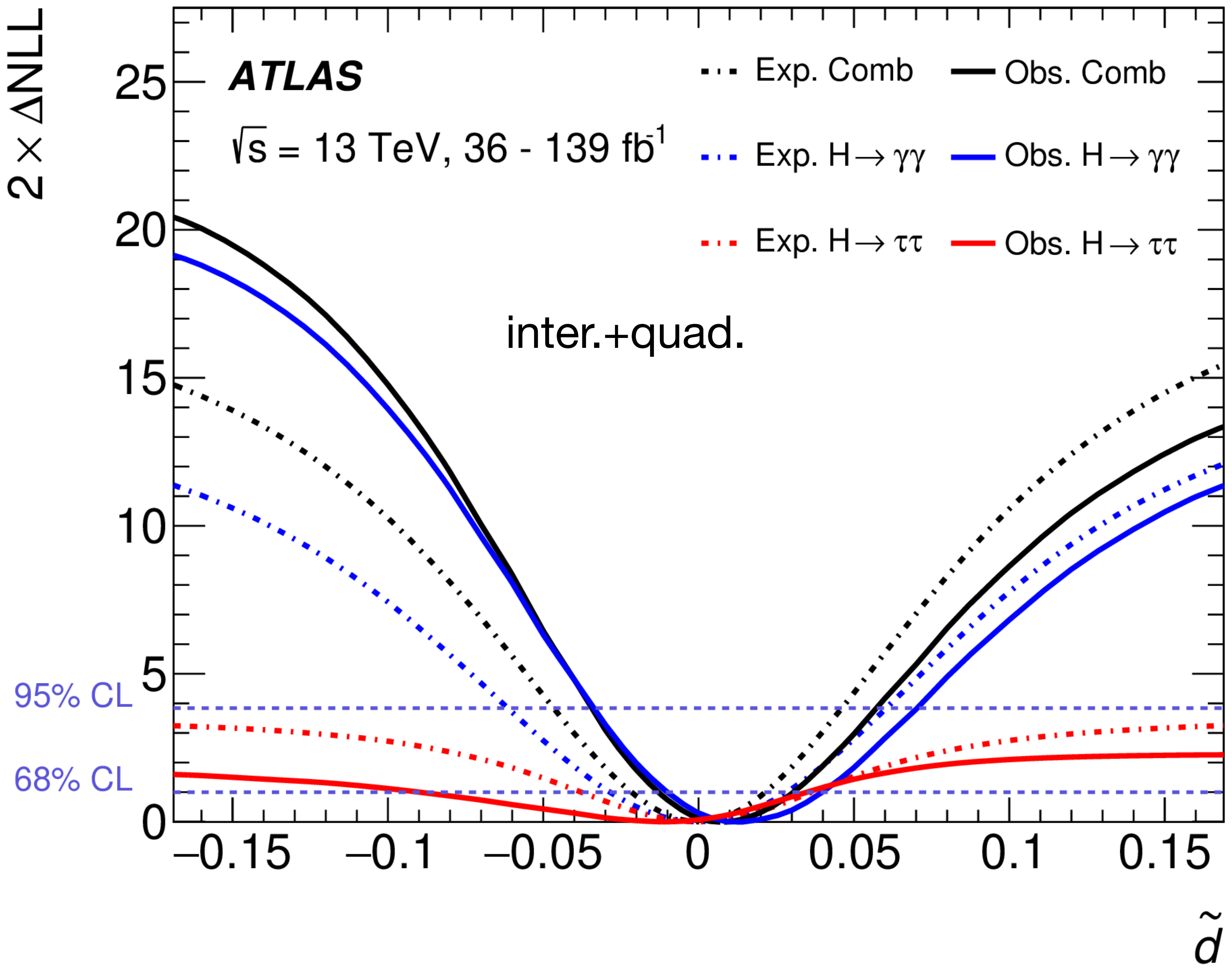

	68% (exp.)	95% (exp.)	68% (obs.)	95% (obs.)
$\tilde{d}$ (inter. only)	[−0.027, 0.027]	[−0.055, 0.055]	[−0.011, 0.036]	[−0.032, 0.059]
$\tilde{d}$ (inter.+quad.)	[−0.028, 0.028]	[−0.061, 0.060]	[−0.010, 0.040]	[−0.034, 0.071]
$\tilde{d}$ from $H \to \tau\tau$	[−0.038, 0.036]	–	[−0.090, 0.035]	-
Combined $\tilde{d}$	[−0.022, 0.021]	[−0.046, 0.045]	[−0.012, 0.030]	[−0.034, 0.057]
$c_{H\tilde{W}}$ (inter. only)	[−0.48, 0.48]	[−0.94, 0.94]	[−0.16, 0.64]	[−0.53, 1.02]
$c_{H\tilde{W}}$ (inter.+quad.)	[−0.48, 0.48]	[−0.95, 0.95]	[−0.15, 0.67]	[−0.55, 1.07]

$\tilde{d}$ (inter.+quad.):
- limits tightened by ~20% for 68% CL
- 3 times better results for 95% CL

$c_{H\tilde{W}}$ (inter. only): 2-5 times more restrictive

previous $H \to \tau\tau$ result Phys. Lett. B 805 (2020) 135426

previous $H \to \gamma\gamma$ result arXiv:2202.00487v3

previous $H \to Z^*Z \to 4\ell$ result arXiv:2004.03447v3

CP mixing angle measurement

top-Higgs coupling ($t\bar{t}H$ and tH) in $H \rightarrow b\bar{b}$ ATLAS-CONF-2022-016

CP-even and CP-odd components

$$\mathscr{L}_{t\bar{t}H} = -\kappa_t' y_t \phi \bar{\psi}_t (\cos\alpha + i\gamma_5 \sin\alpha)\psi_t$$

best-fit value $\alpha = 11^{\circ}{}^{+56^\circ}_{-77^\circ}$, $\kappa_t' = 0.83^{+0.30}_{-0.46}$

pure CP-odd coupling disfavoured at 1.2 standard deviation

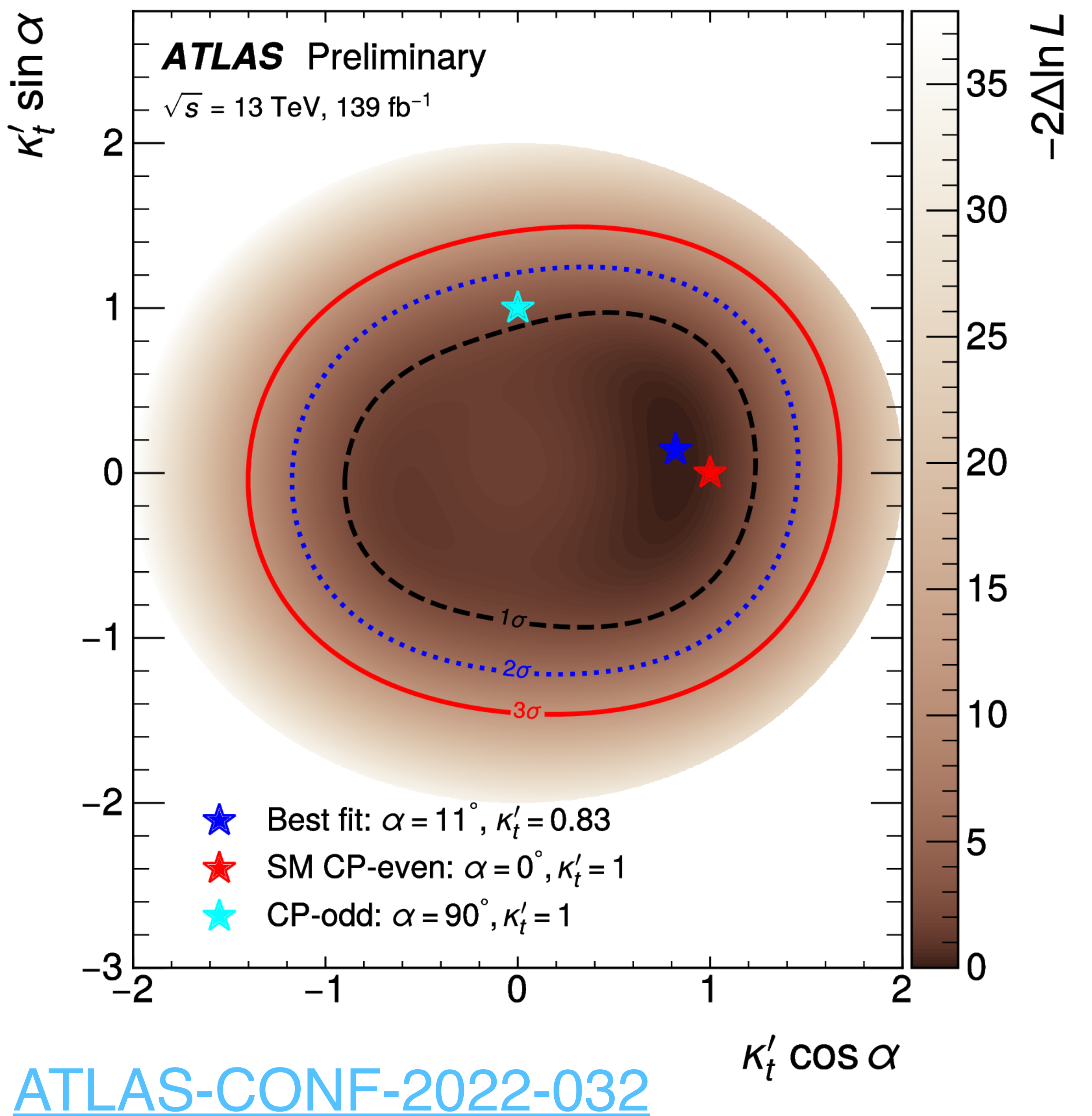

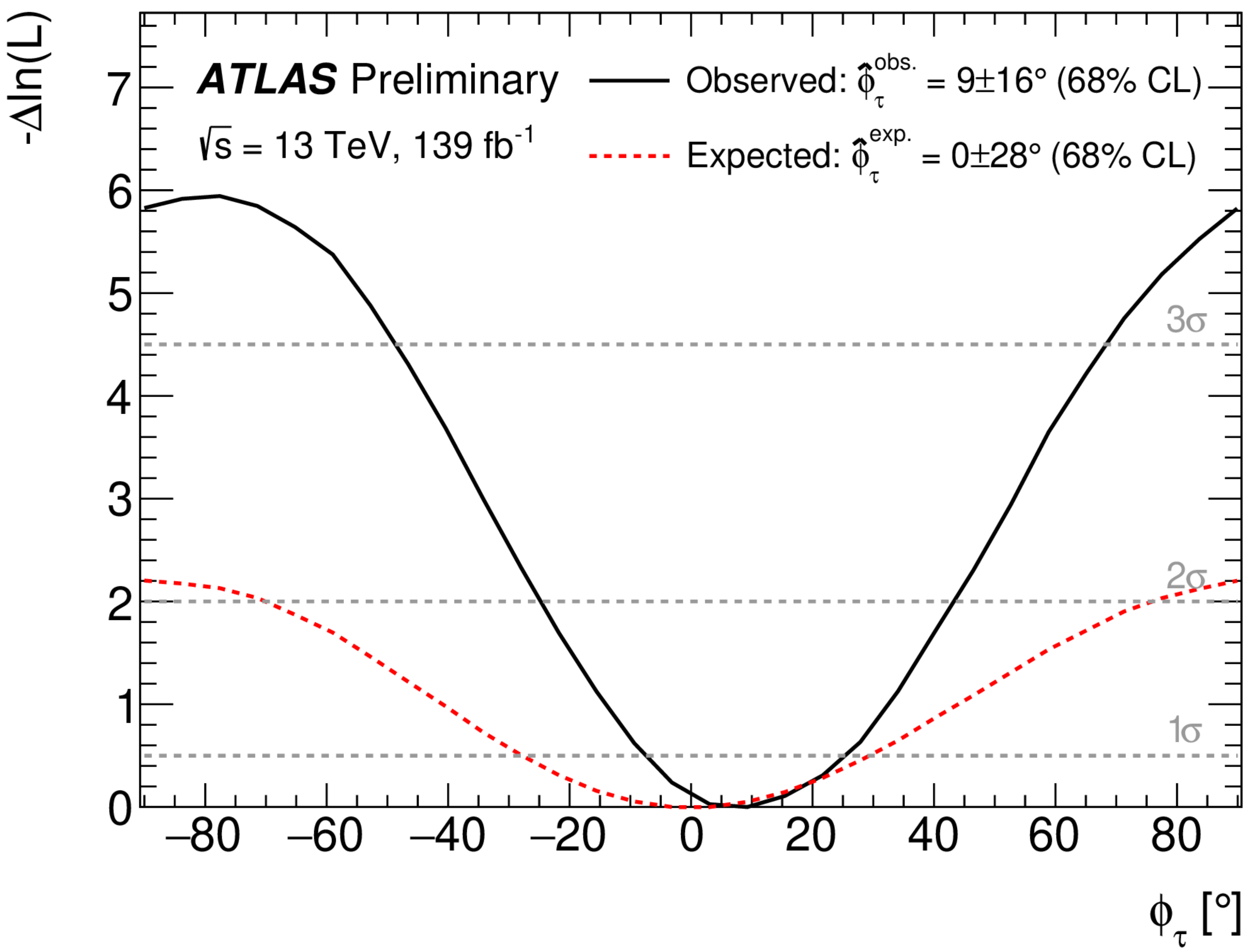

τ-Higgs coupling in $H \rightarrow \tau\tau$ ATLAS-CONF-2022-032

CP-even and CP-odd components

$$\mathscr{L}_{H\tau\tau} = -\frac{m_\tau}{v}\kappa_t(\cos\phi_\tau \bar{\tau}\tau + \sin\phi_\tau \bar{\tau} i\gamma_5 \tau)H$$

Exclusion of CP-odd hypothesis at 3.4 standard deviation

Simplified template cross-section

[arXiv:2207.00348v1](https://arxiv.org/abs/2207.00348v1)

$H \rightarrow \gamma\gamma$

Optimised to simultaneously measure cross-sections in 28 Higgs boson phase space regions in 101 categories

- splitting in STXS bins based on kinematics
- non-overlapping fiducial regions

BDT classifier for signal separation among the various STXS regions

Binary multivariate classifier to separate signal from continuum background and improve measurement sensitivity

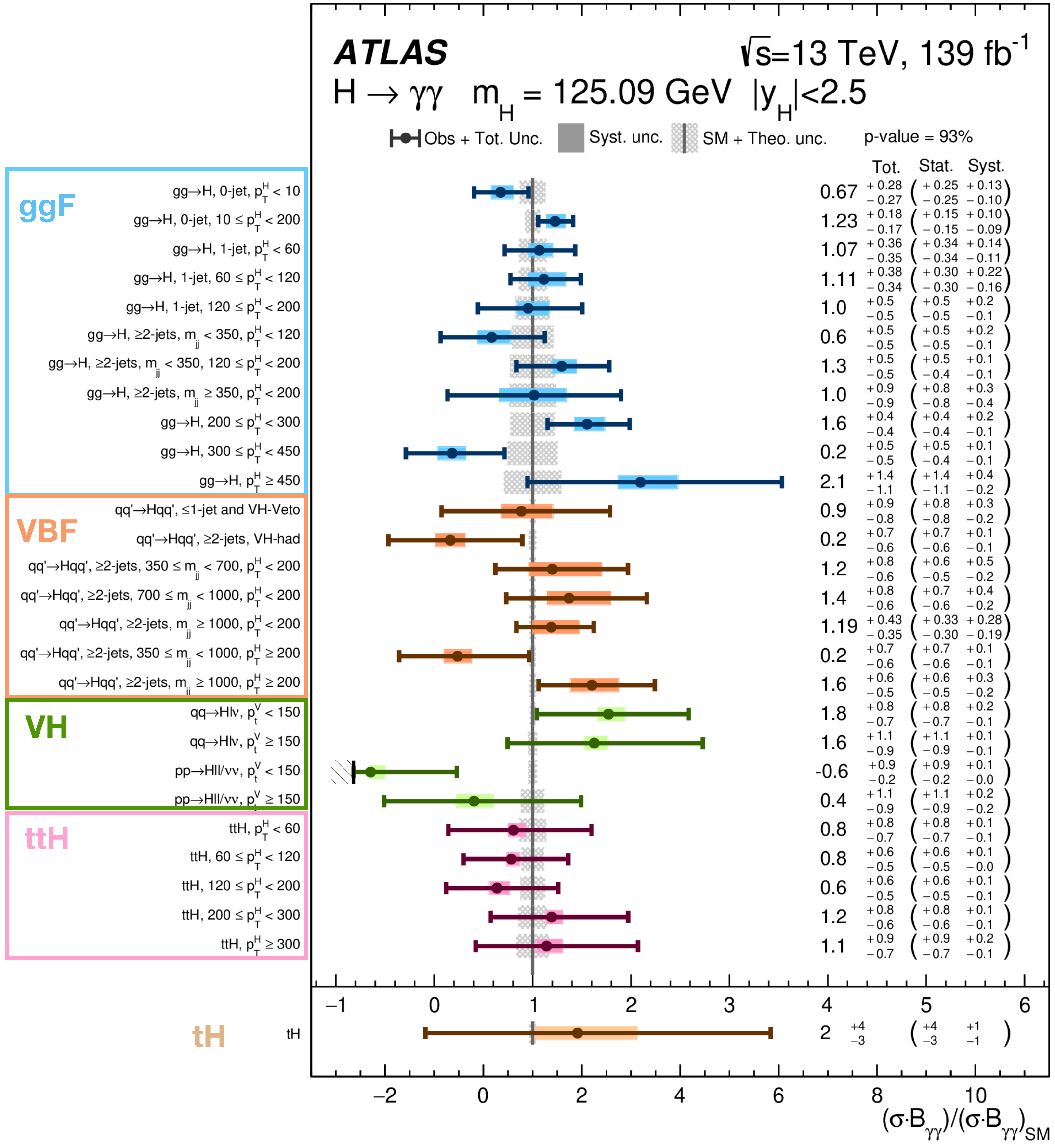

No significant deviation from SM

EFT interpretation

arXiv:2207.00348v1

$\underline{H \rightarrow \gamma\gamma}$

33 STXS regions (finer selection)

34 Wilson coefficients in Warsaw basis free to vary in the fit

each STXS region affected by multiple operators

Principal component analysis

compute eigenvectors EVn

$$C^{-1}_{\mathrm{SMEFT}} = P^T C^{-1}_{STXS} P$$

align measurement with the eigenvectors

→ unconstrained eigenvectors are fixed to 0

→ 12 eigenvectors in the fit

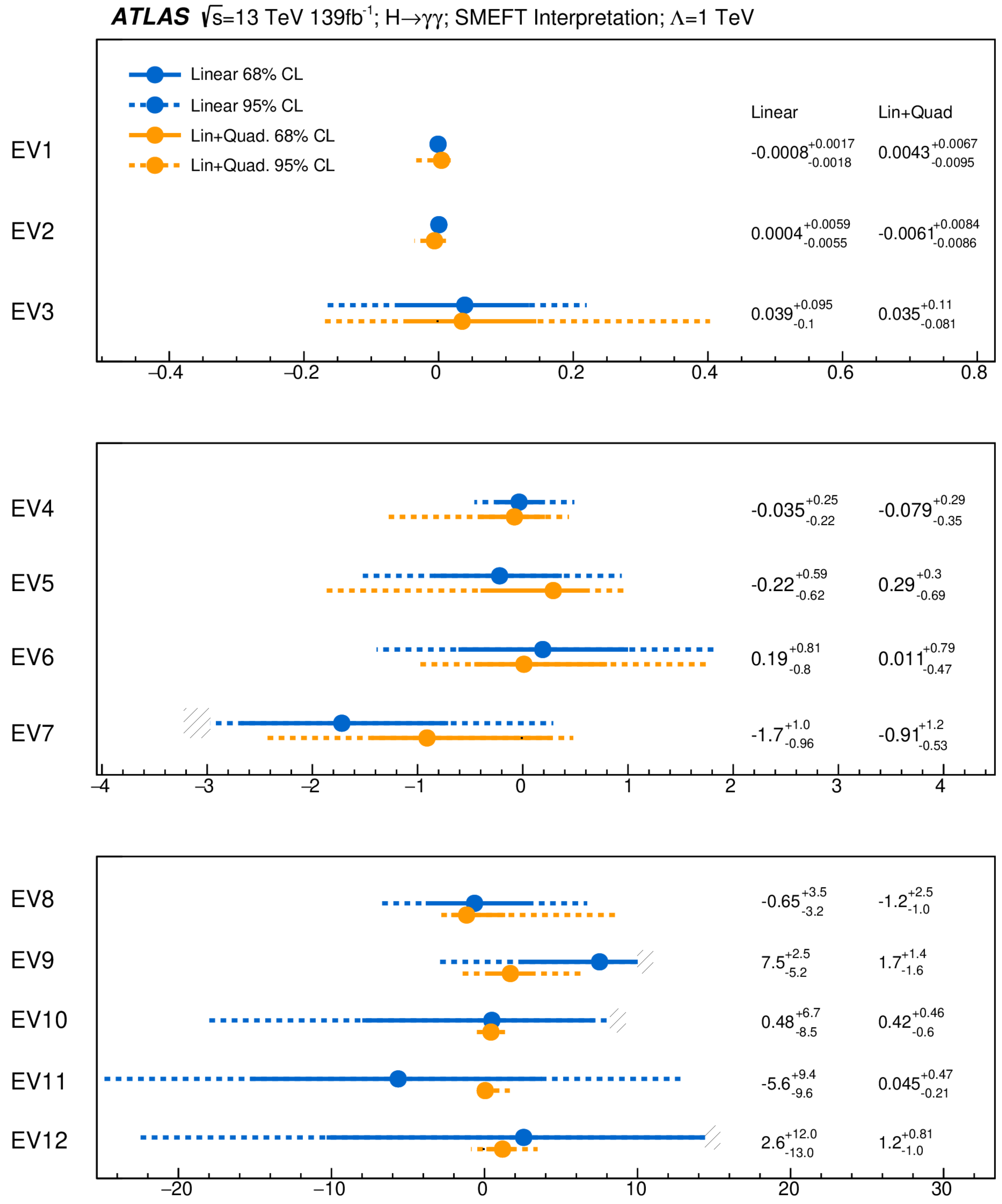

No significant deviation from SM

Differential cross sections measurements

arXiv:2207.08615v1

$H \to \gamma\gamma$ and $H \to ZZ^* \to 4\ell$

Individual channels: measurements in fiducial regions
to reduce signal model dependence

Combination: extrapolation to the full phase space

single and double differential cross-sections for
- Higgs boson p_T
- Higgs boson $|y_H|$
- jet multiplicity
- leading jet p_T

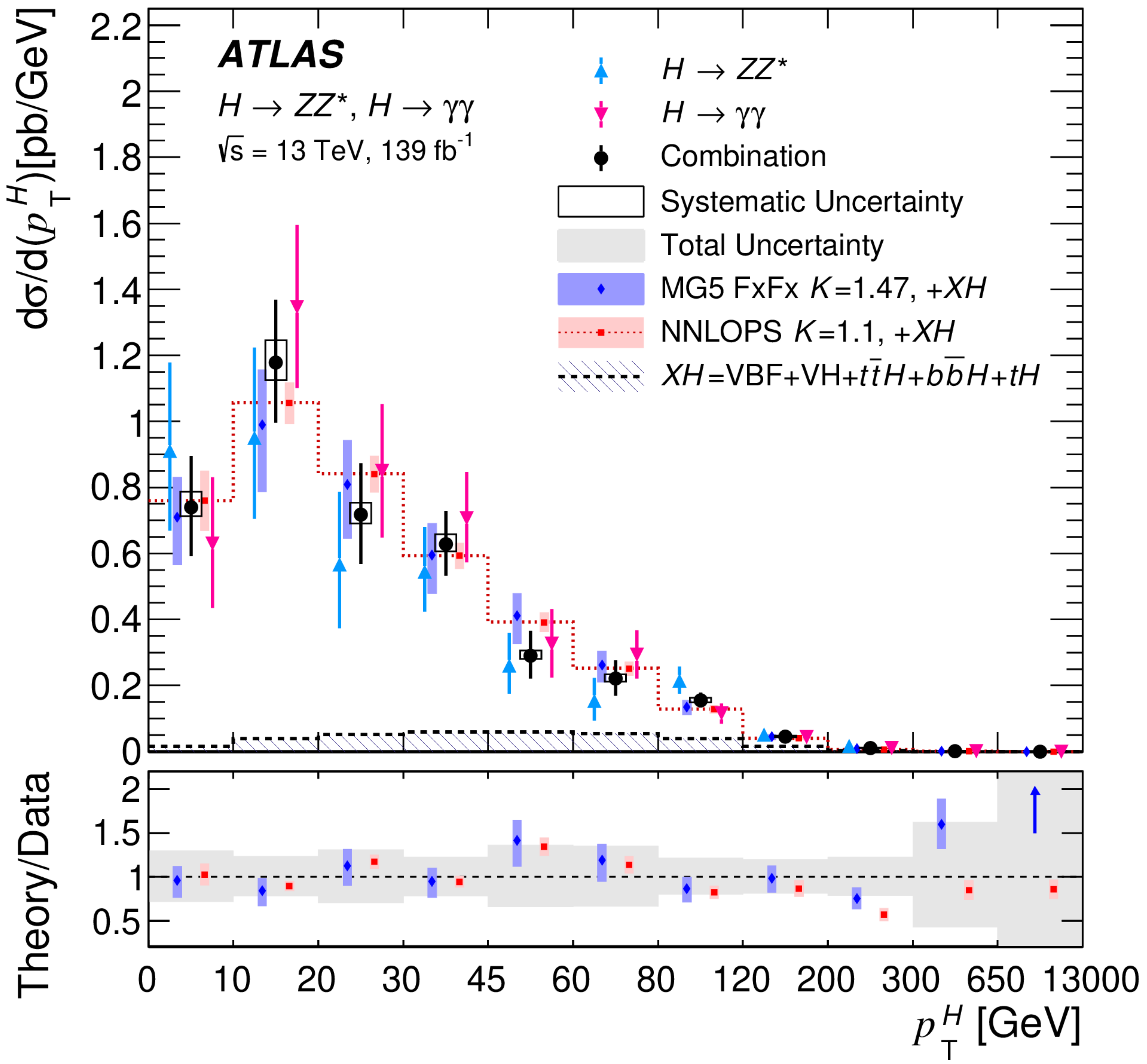

Results compatible with SM

~20-30% precision up to 300 GeV

~60% precision in 300-650 GeV

Couplings combining measurement

arXiv:2207.00092v1

Simultaneous fit of cross-section × branching fraction for the individual measurement

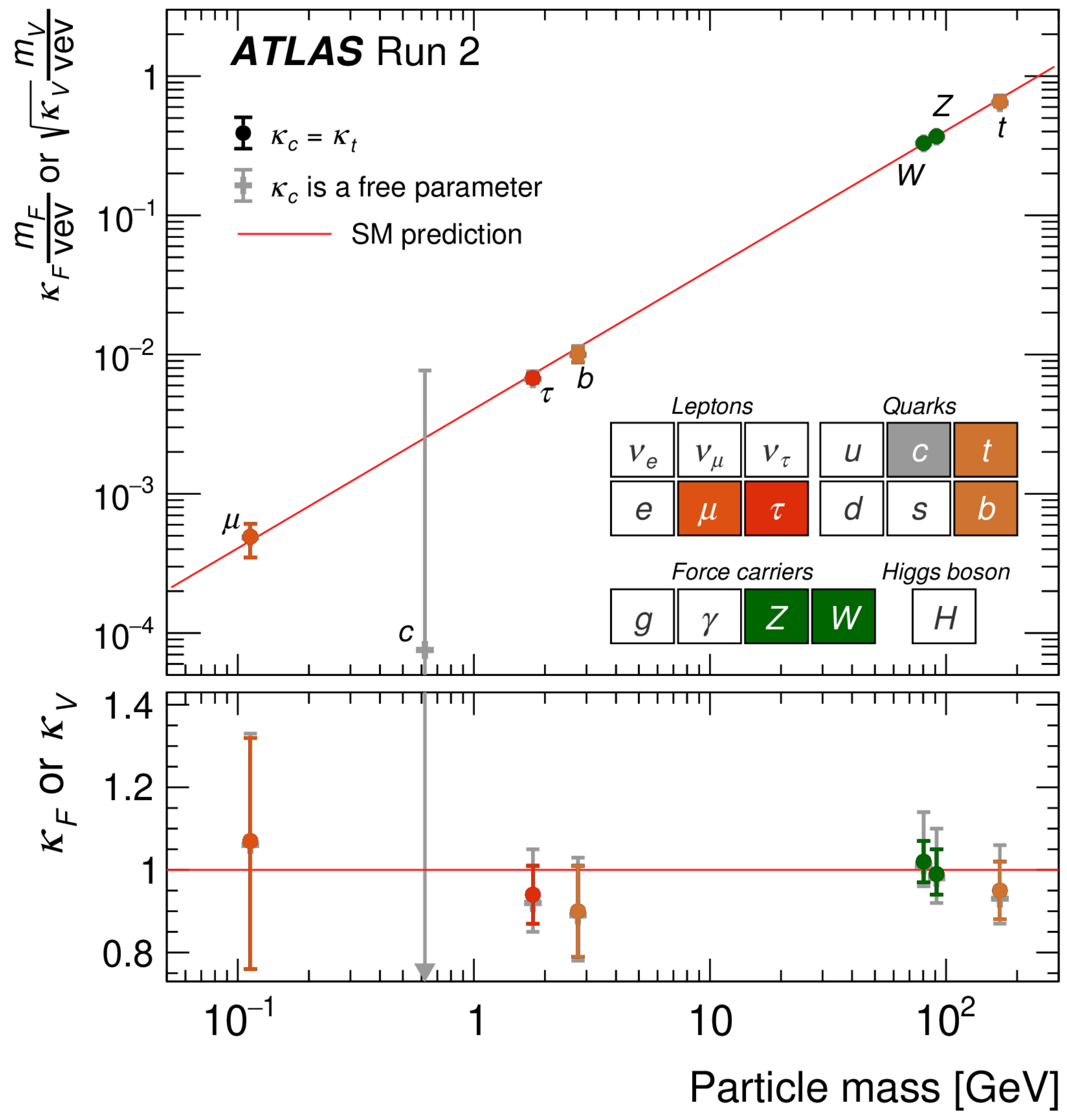

Parametrisation in κ-framework

$$\sigma(i \to H \to f) = \sigma_i B_f = \frac{\sigma_i(\kappa)\Gamma_f(\kappa)}{\Gamma_H(\kappa, B_{inv}, B_u)}$$

all decay modes

direct or indirect SM decays

hypothetical decays into non-SM particles

Results compatible with SM

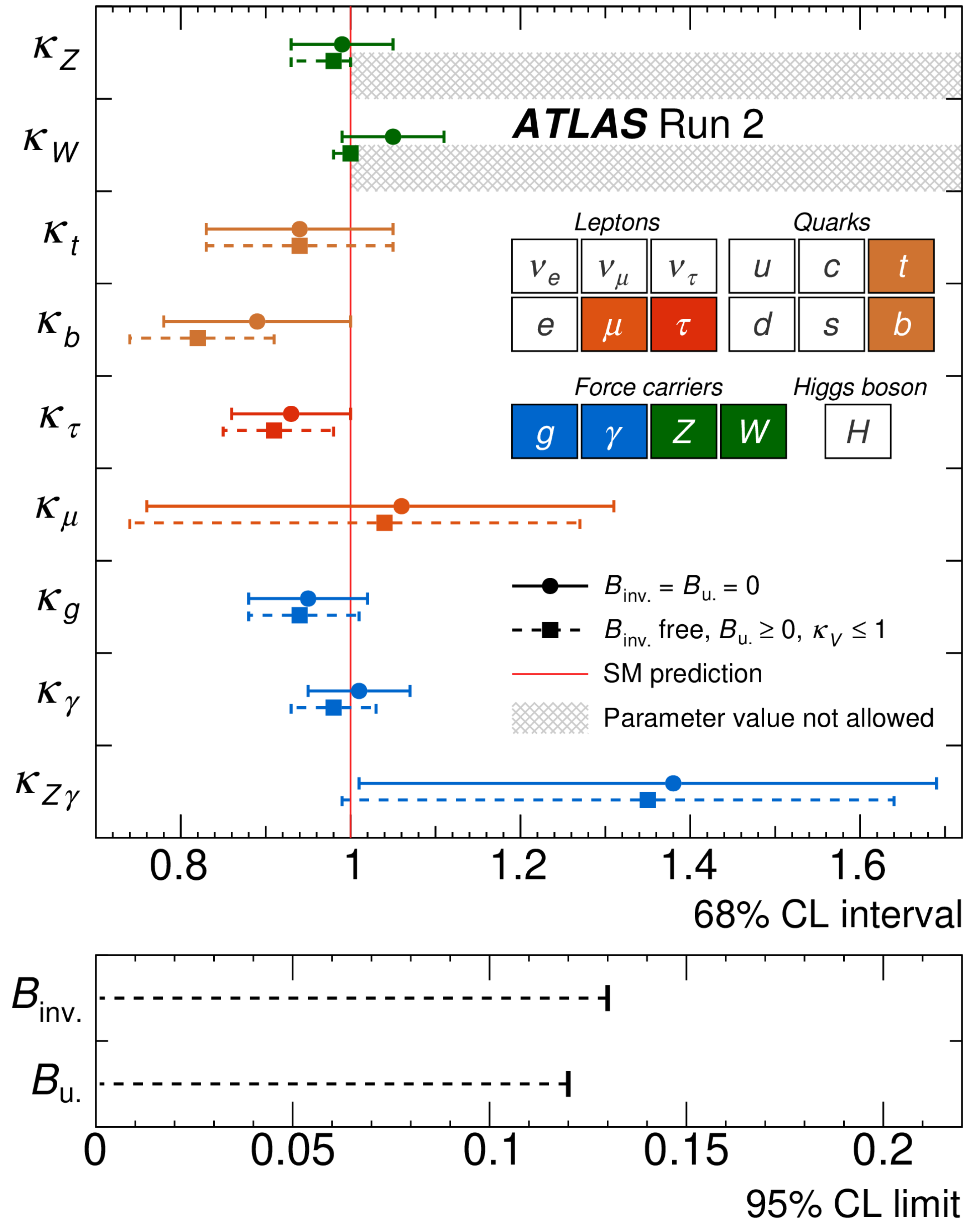

unconstrained scenario put an improved limit w.r.t arXiv:2201.11428v4
$\kappa_c < 5.7\ (6.7)$ times SM obs. (exp.) at 95% CL

better limit achieved w.r.t direct searches arXiv:2202.07953v2

Higgs self-coupling

ATLAS-CONF-2022-050

SM: $V(H) = \frac{1}{2} m_{\mathrm{H}}^2 H^2 + \lambda_{\mathrm{HHH}} v H^3 + \frac{1}{4} \lambda_{\mathrm{HHHH}} H^4$, $\kappa_\lambda = \frac{\lambda_{\mathrm{HHH}}}{\lambda_{\mathrm{HHH}}^{SM}}$

Direct measurements: production of two Higgs bosons

gluon-gluon Fusion: $\sigma_{ggF}^{SM}(pp \to HH) \simeq 31.0$ fb

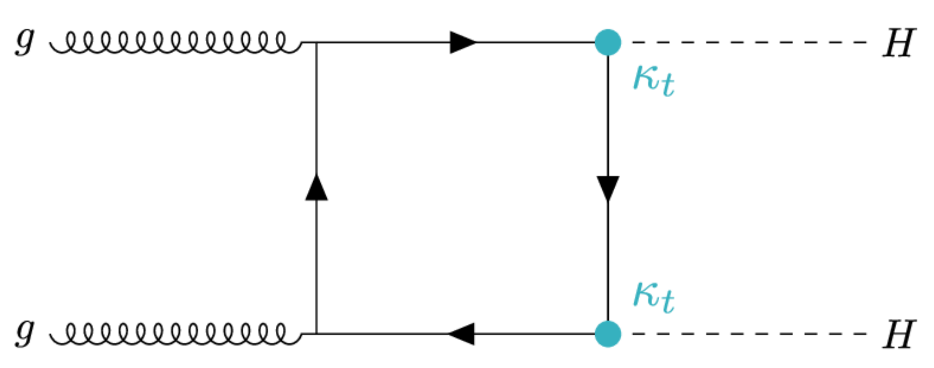

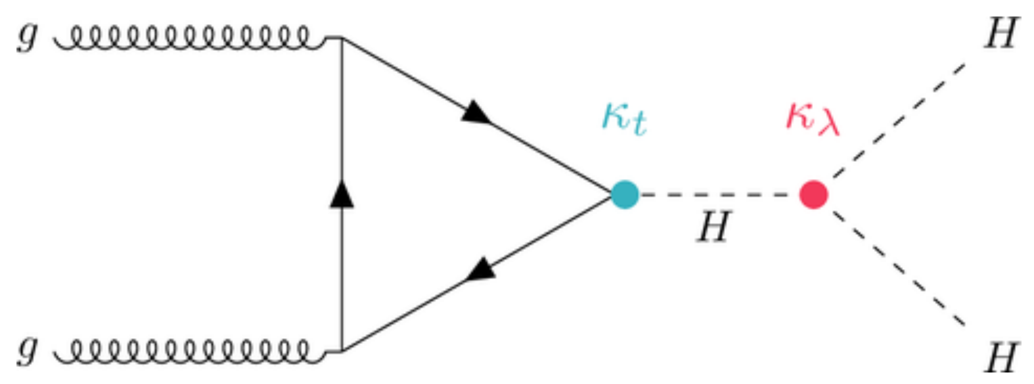

Vector Boson Fusion: $\sigma_{VBF}^{SM}(pp \to HH) \simeq 1.72$ fb

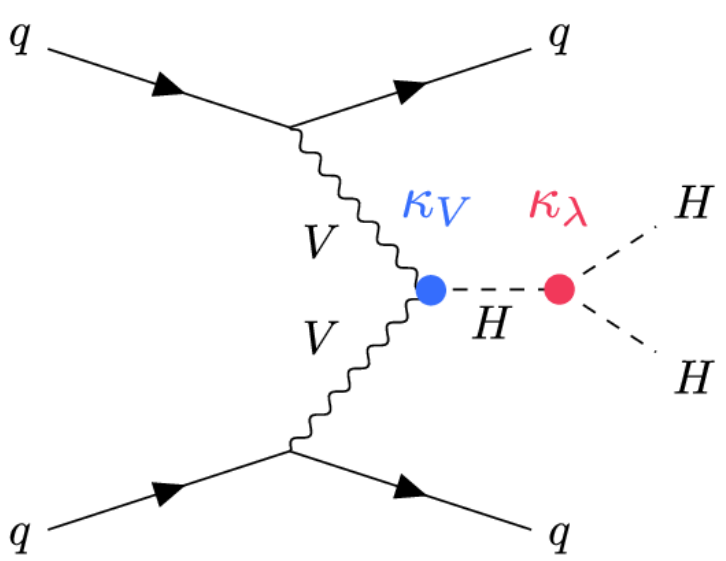

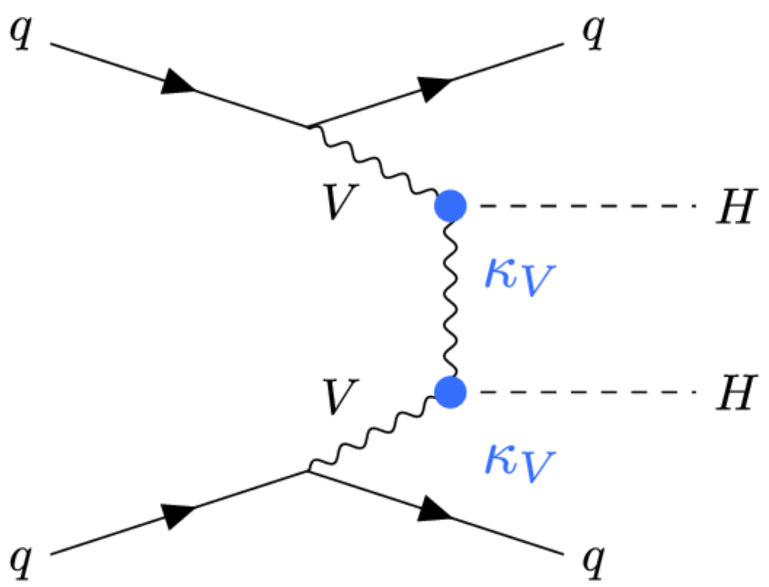

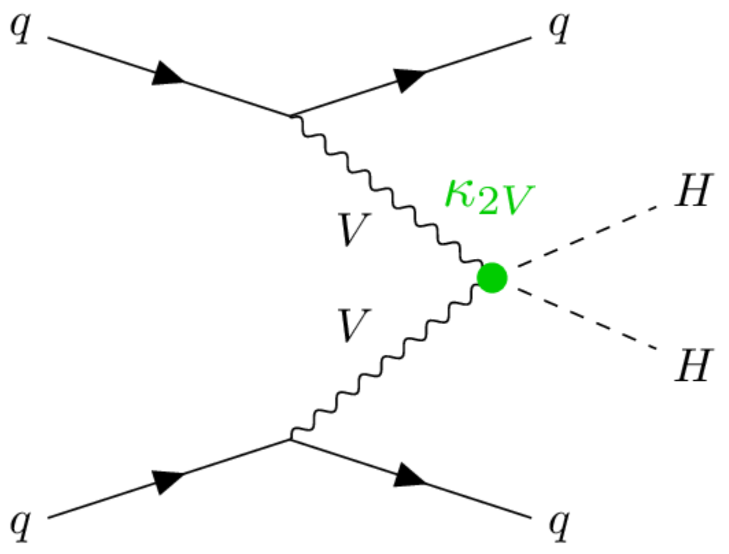

Indirect measurements: single-Higgs production

Higgs boson self-energy

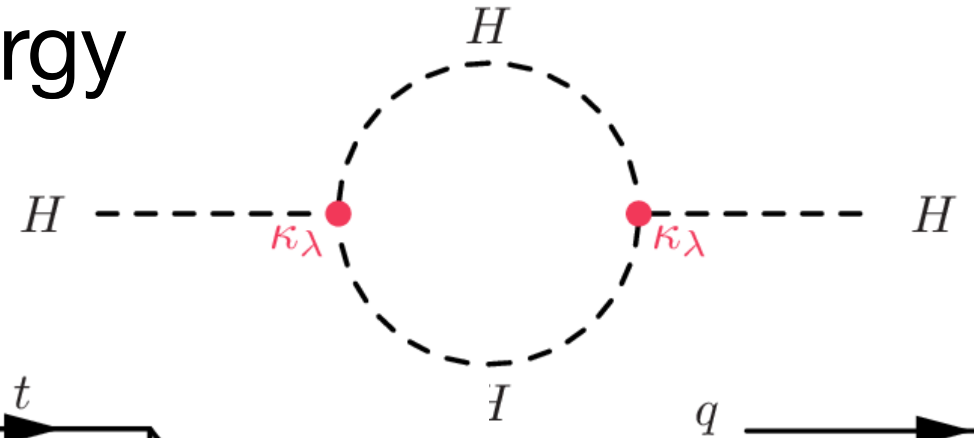

Production modes

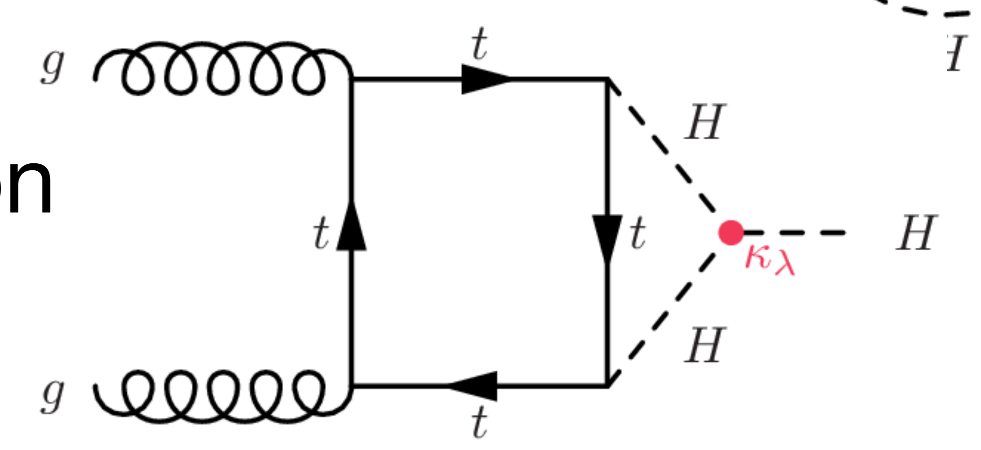

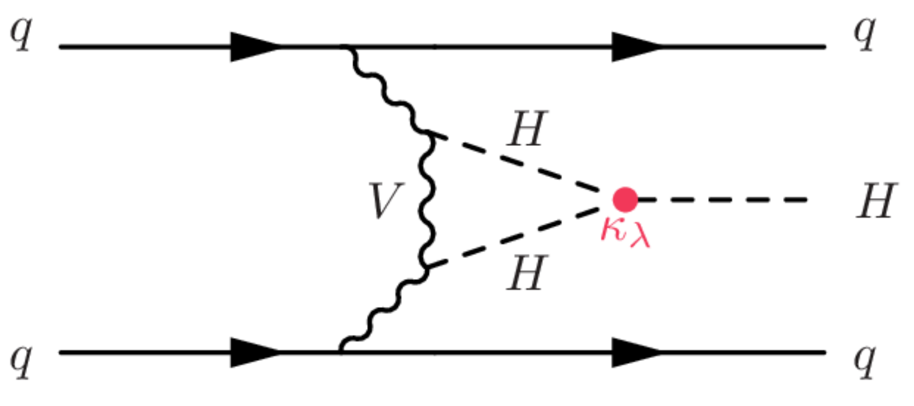

Decays

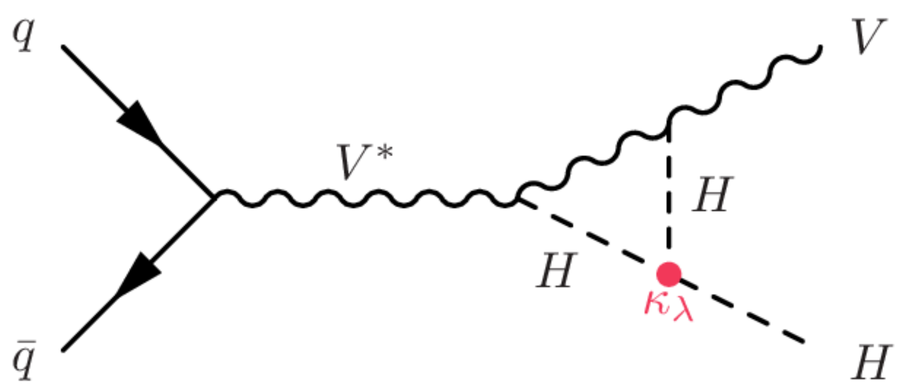

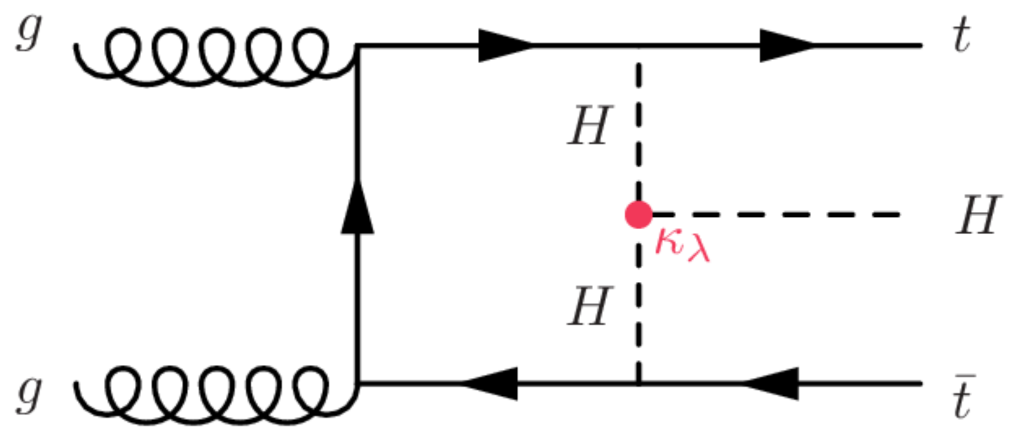

Any deviation from the self-interaction predicted by the SM would be a sign of new physics

Higgs self-coupling

ATLAS-CONF-2022-050

Two tested scenarios:

κ_λ *only*: κ_λ floating & all other modifiers fixed to unity

κ_λ *generic*: $\kappa_\lambda, \kappa_t, \kappa_b, \kappa_\tau, \kappa_V$ floating & κ_{2V} fixed to unity (no available parametrisation of single-Higgs NLO)

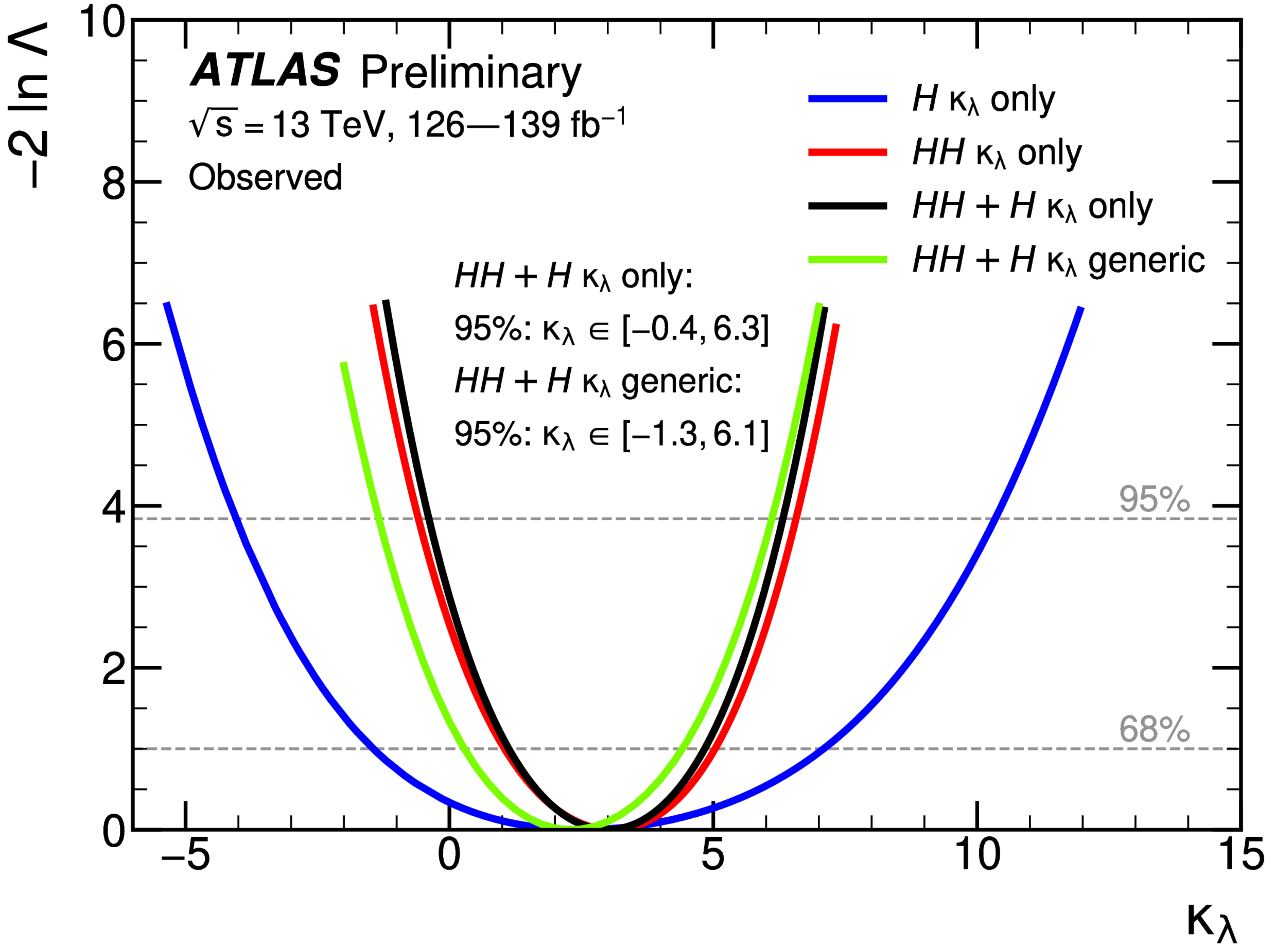

Combination assumption	Obs. 95% CL	Exp. 95% CL	Obs. value$^{+1\sigma}_{-1\sigma}$
HH combination	$-0.6 < \kappa_\lambda < 6.6$	$-2.1 < \kappa_\lambda < 7.8$	$\kappa_\lambda = 3.1^{+1.9}_{-2.0}$
Single-H combination	$-4.0 < \kappa_\lambda < 10.3$	$-5.2 < \kappa_\lambda < 11.5$	$\kappa_\lambda = 2.5^{+4.6}_{-3.9}$
HH+H combination	$-0.4 < \kappa_\lambda < 6.3$	$-1.9 < \kappa_\lambda < 7.5$	$\kappa_\lambda = 3.0^{+1.8}_{-1.9}$
HH+H combination, κ_t floating	$-0.4 < \kappa_\lambda < 6.3$	$-1.9 < \kappa_\lambda < 7.6$	$\kappa_\lambda = 3.0^{+1.8}_{-1.9}$
HH+H combination, κ_t, κ_V, κ_b, κ_τ floating	$-1.3 < \kappa_\lambda < 6.1$	$-2.1 < \kappa_\lambda < 7.6$	$\kappa_\lambda = 2.3^{+2.1}_{-2.0}$

Summary

- We have studied the Higgs boson properties with great precision since its discovery
- Improvement of the analysis techniques
- Higgs boson nature consistent with the SM predictions
- Ample room for new phenomena BSM to be discovered
- Looking forward to Run 3 data to reach higher sensitivity to potential new physics
  Expect to profit from latest detector developments

Thank you for the attention!

Backup

Mass measurement

arXiv:2207.00320v1

$H \rightarrow ZZ^* \rightarrow 4\ell$

Final states: 4μ, $2e2\mu$, $2\mu 2e$, $4e$

1 quadruplet per event

Final-state radiation (FSR) γ

1 FSR candidate per quadruplet

$m_{4\ell}$ resolution improvement by ~1%

Z-boson mass constraint

$m_{4\ell}$ resolution improvement by ~17%

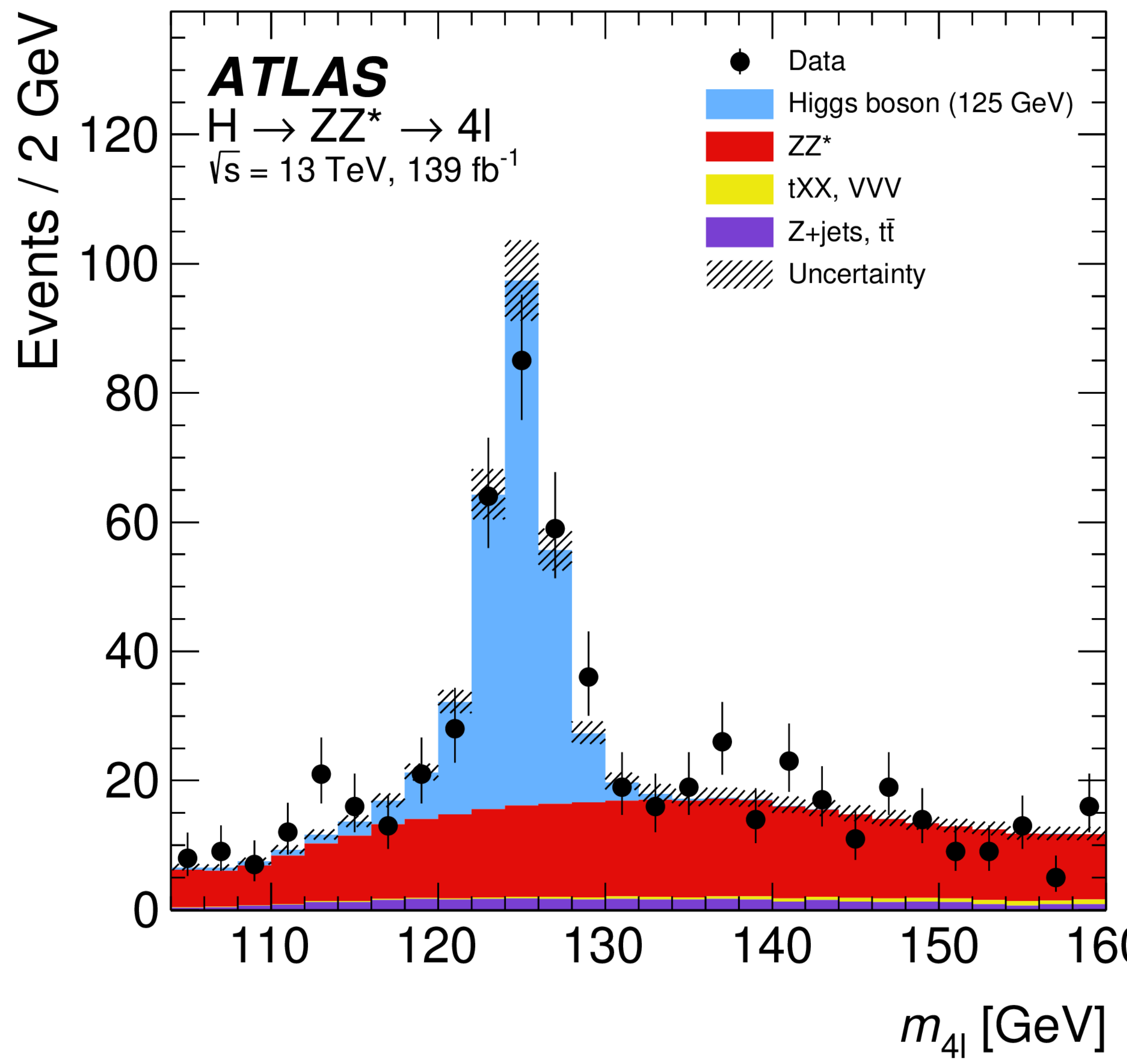

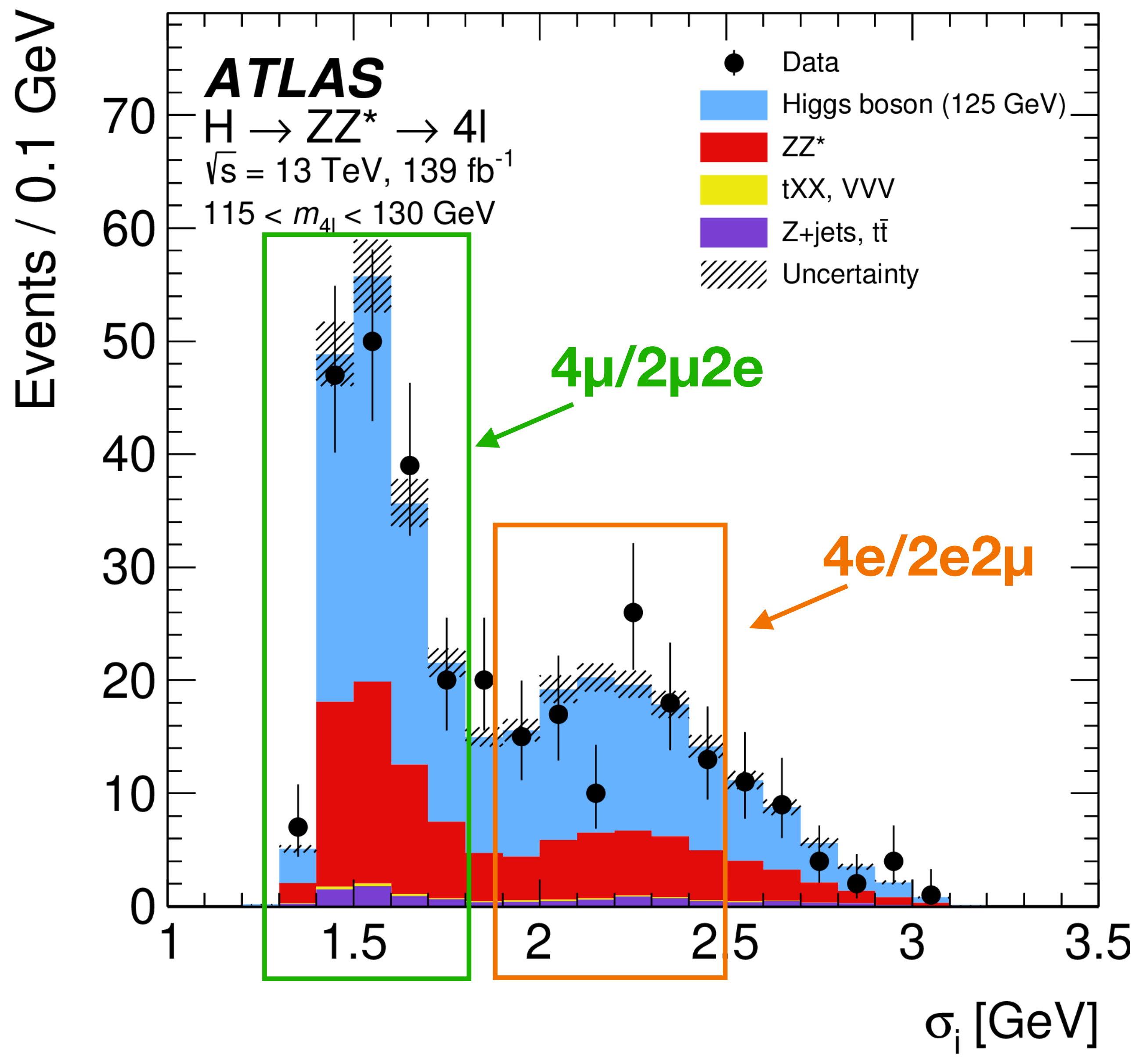

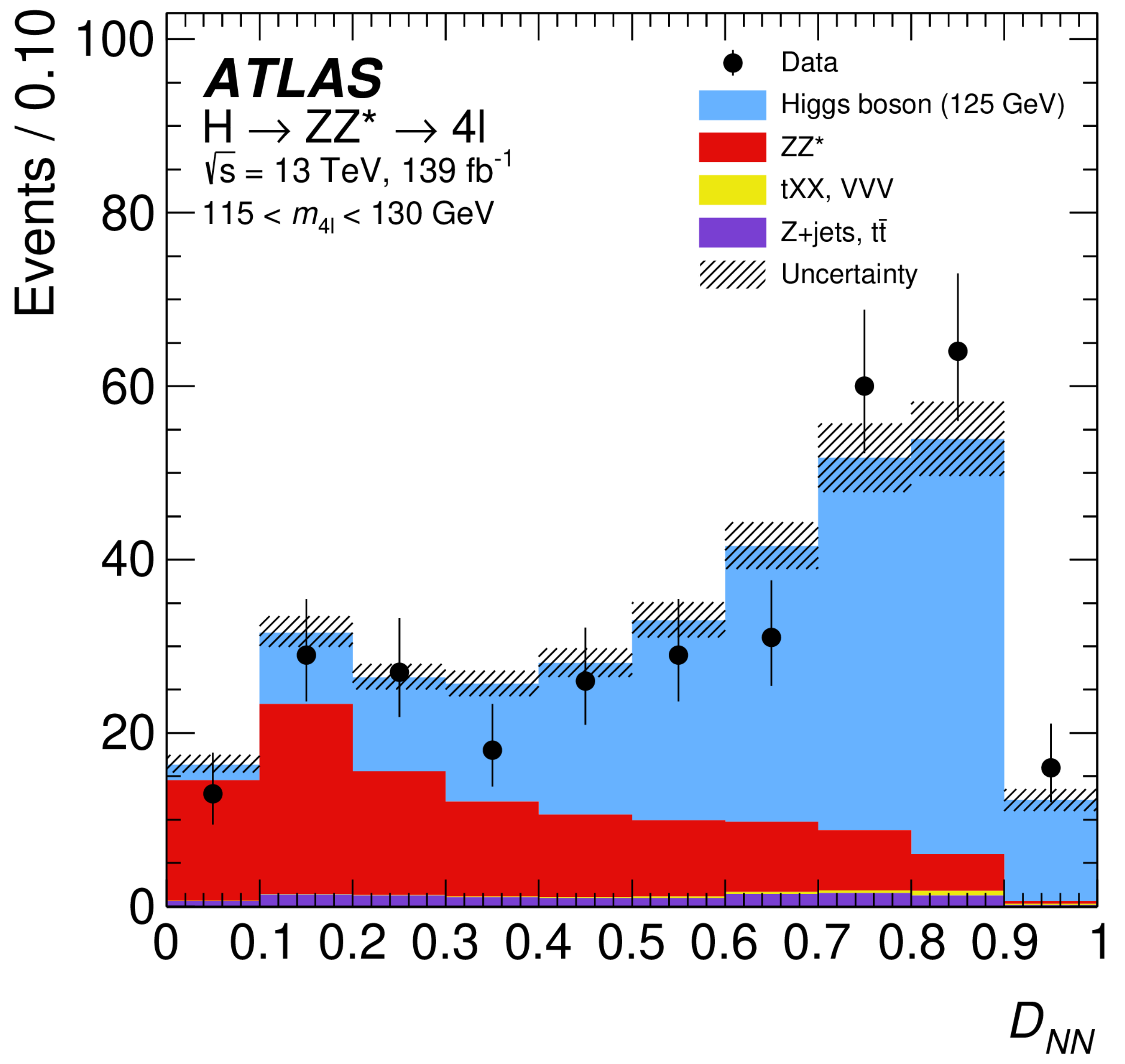

QRNN Inputs:

$p_T^{\ell}, \eta^{\ell}, \phi^{\ell}$ +

constrained $p_T^{4\ell}$ & uncertainty

NN Inputs:

$p_T^{4\ell}, \eta^{4\ell}, \ln(|\mathcal{M}_{HZZ*}|^2/|\mathcal{M}_{ZZ*}|^2)$

CP measurement

arXiv:2208.02338v1

bosonic coupling in VBF $\mathrm{H} \rightarrow \gamma\gamma$ channel

Optimal Observable method - $OO = 2 \cdot \mathrm{Re}(\mathscr{M}^*_{\mathrm{SM}} \cdot \mathscr{M}_{\mathrm{CP-odd}}) / |\mathscr{M}_{\mathrm{SM}}|^2$ using $p_{\mathrm{T}}^{\mathrm{H}}$ and $p_{\mathrm{T}}^{\mathrm{jj}}$

VBF signal: BDT based event categorisation - fit to the $m_{\gamma\gamma}$ split into the *OO* bins

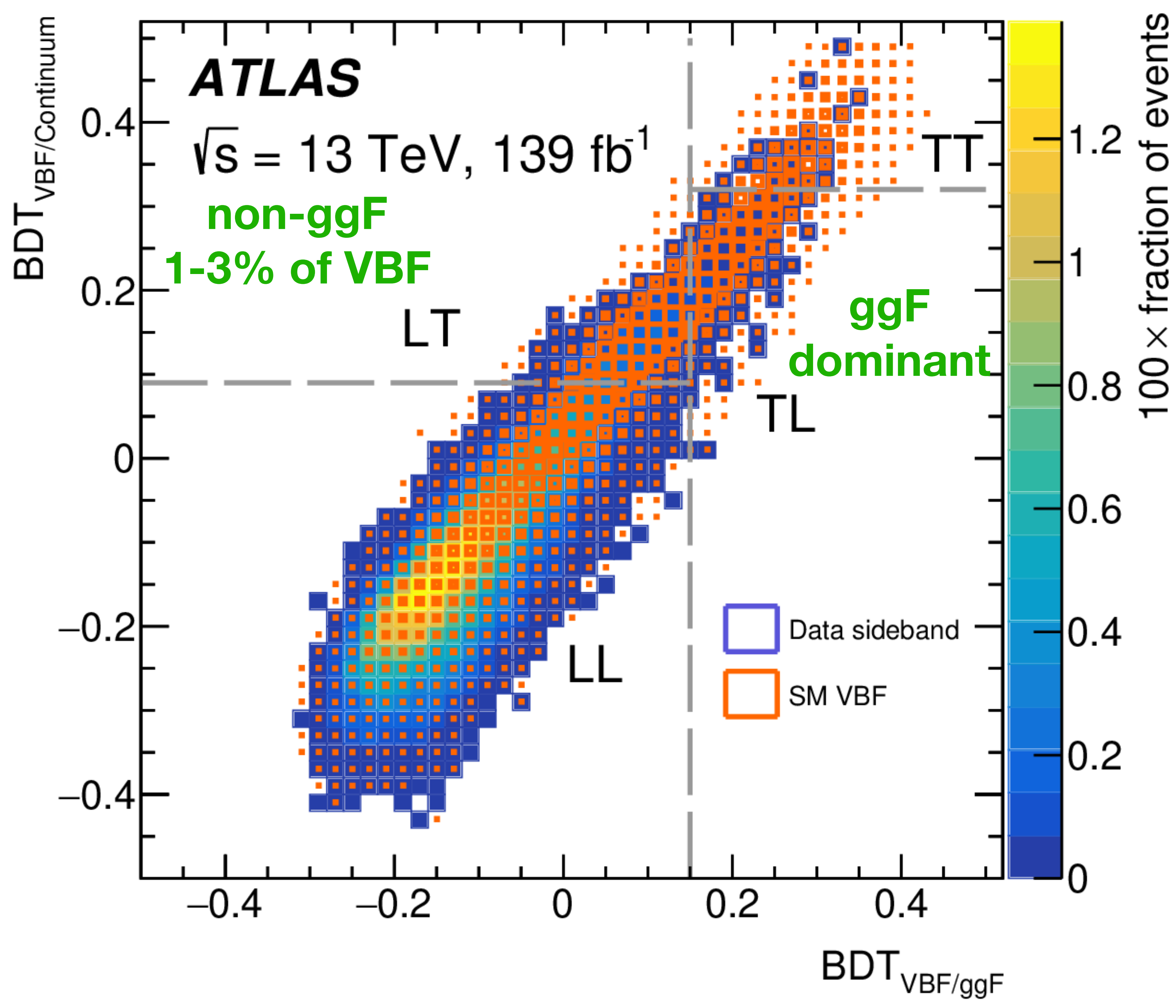

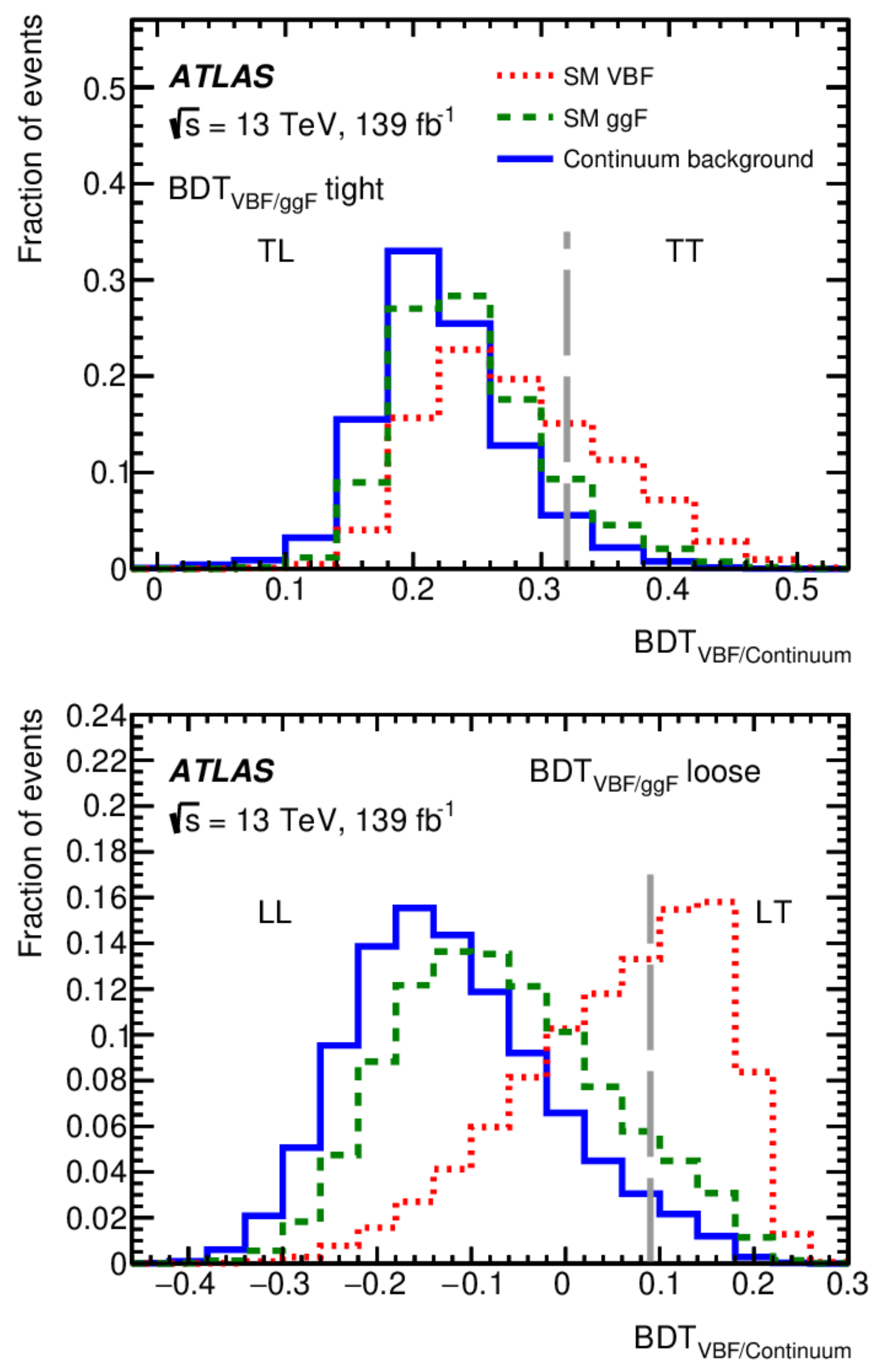

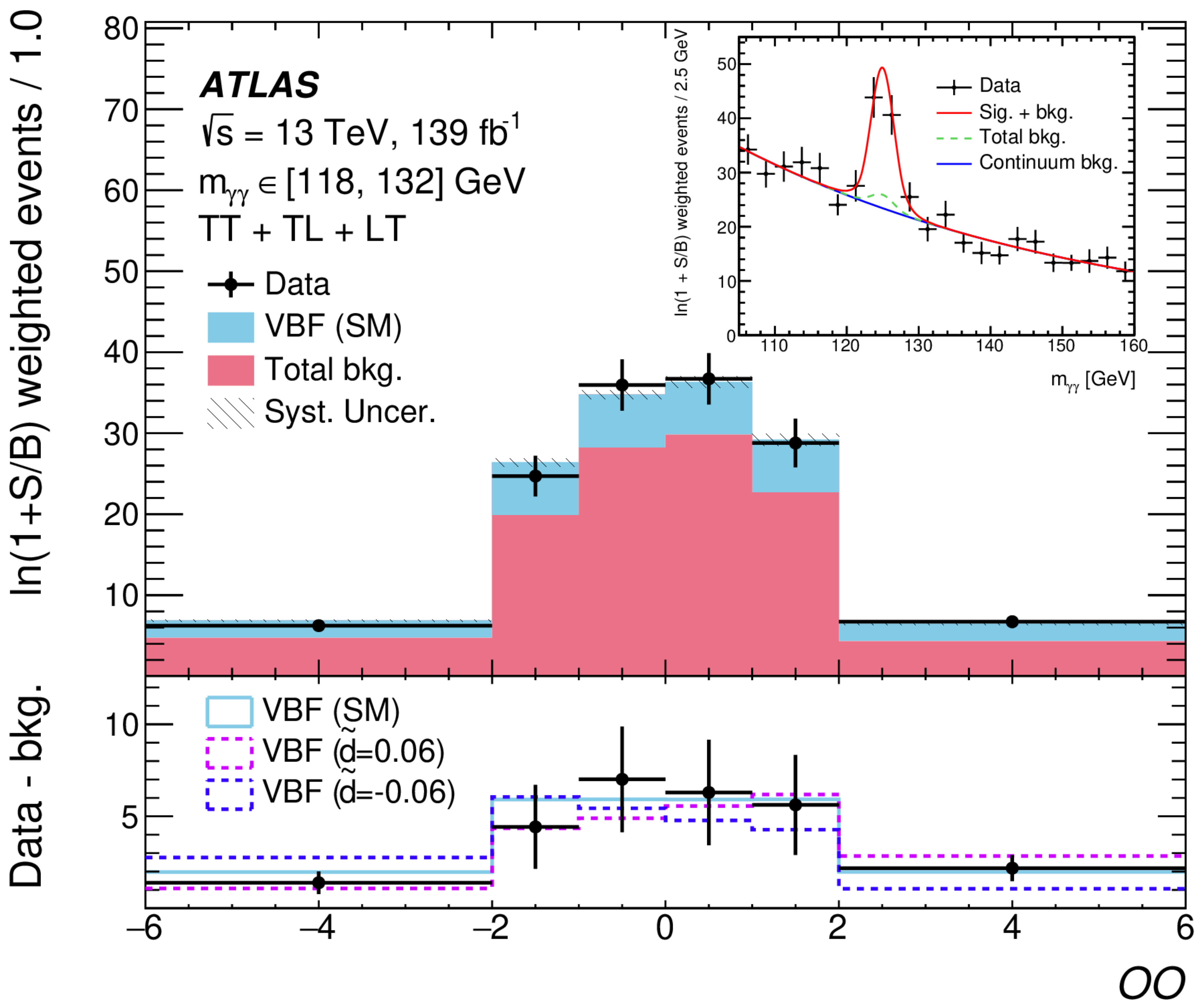

CP measurement

Comparisons with other results

arXiv:2208.02338v1

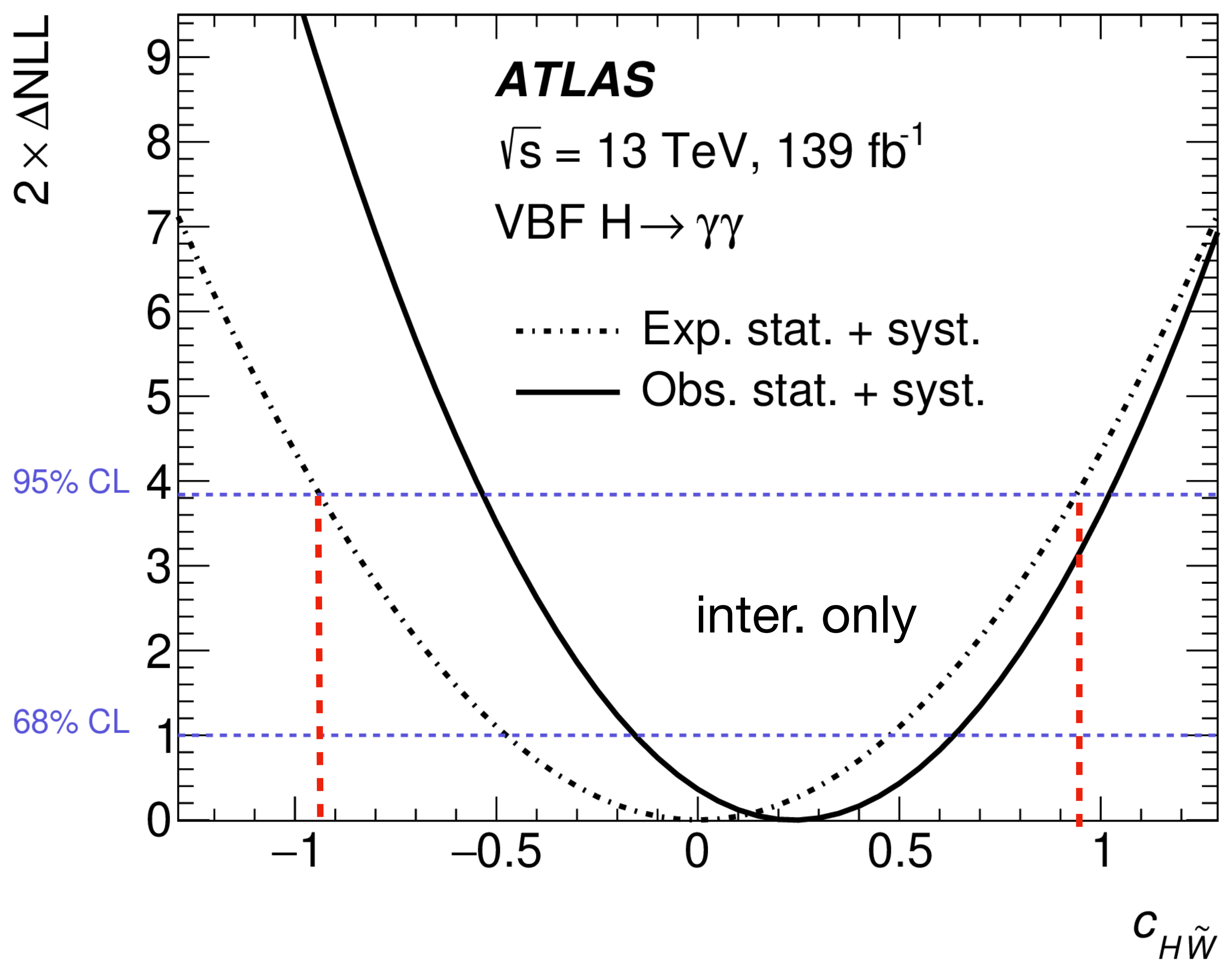

arXiv:2202.00487

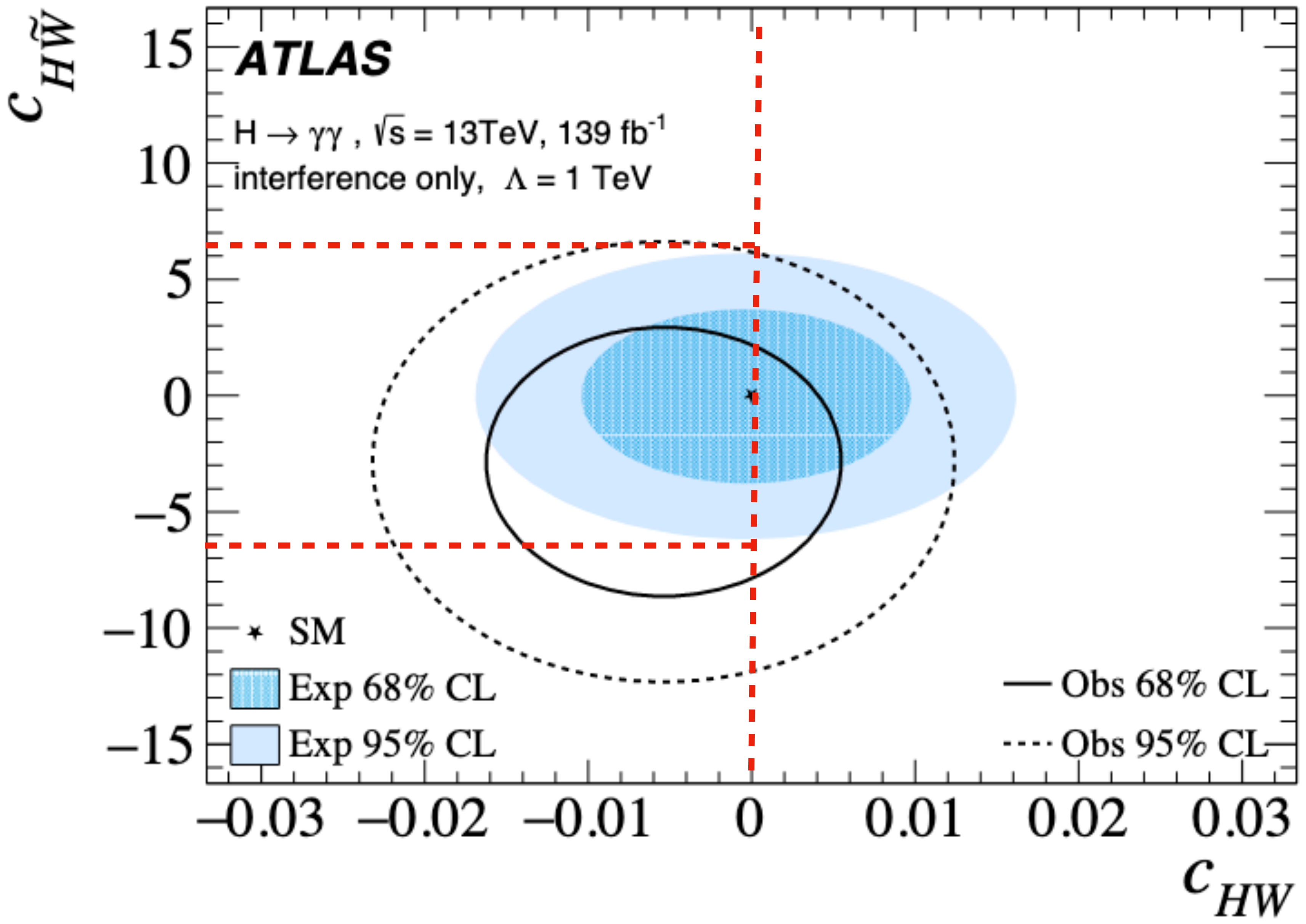

arXiv:2004.03447v3

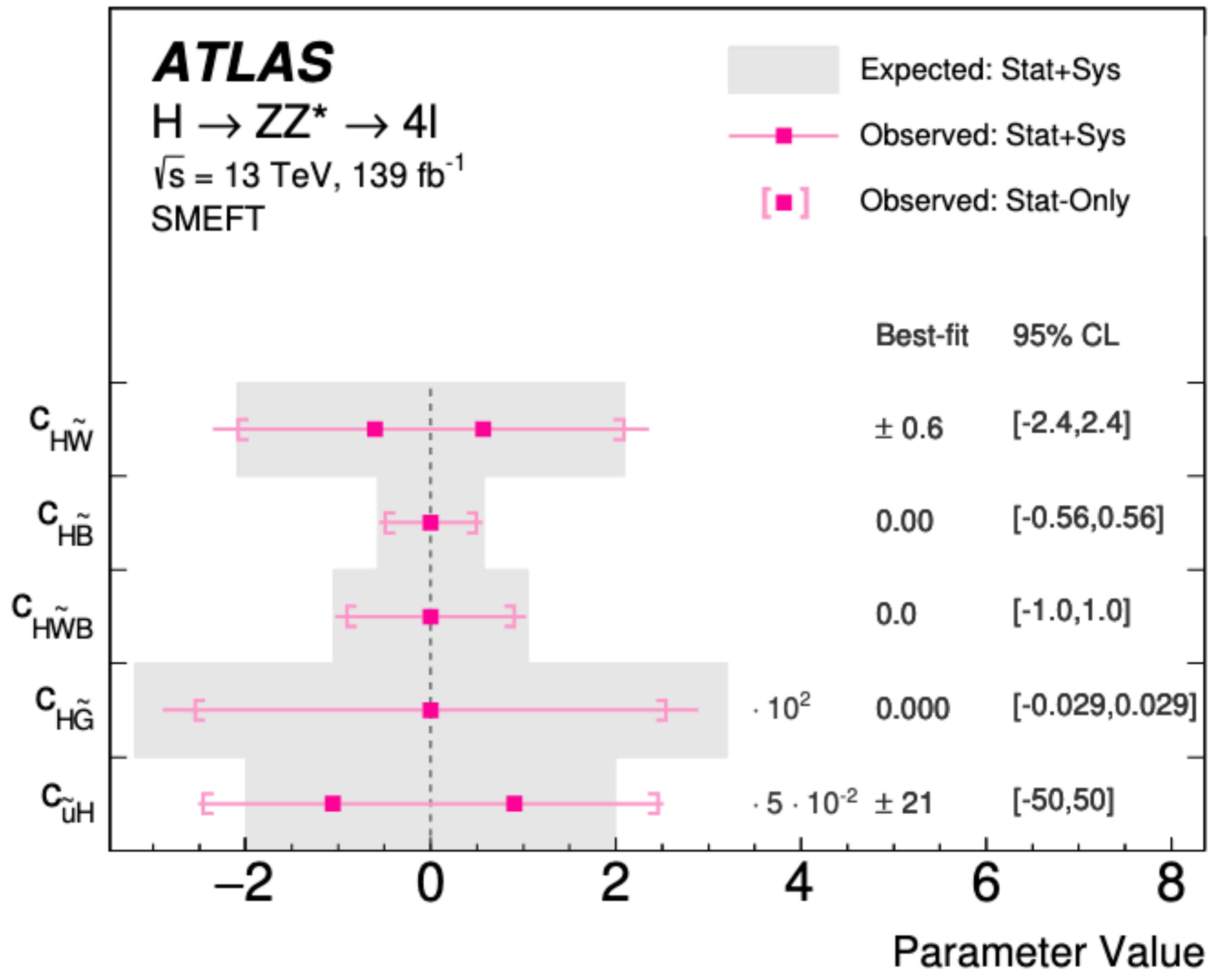

CP mixing angle measurement

top-Higgs coupling ($t\bar{t}H$ and tH) in $H \to b\bar{b}$ ATLAS-CONF-2022-016

Signal: $t\bar{t}H$ and tH events

Final states: at least 1 top quark decays semi-leptonically to e/μ

ℓ+jets and dilepton channels

Background dominated by $t\bar{t}$+jets

Event categorisation:

1. Define Control Regions (CR) and Preliminary Signal Regions (PSR)
2. MVA used to define additional CR and final SR from the PSRs

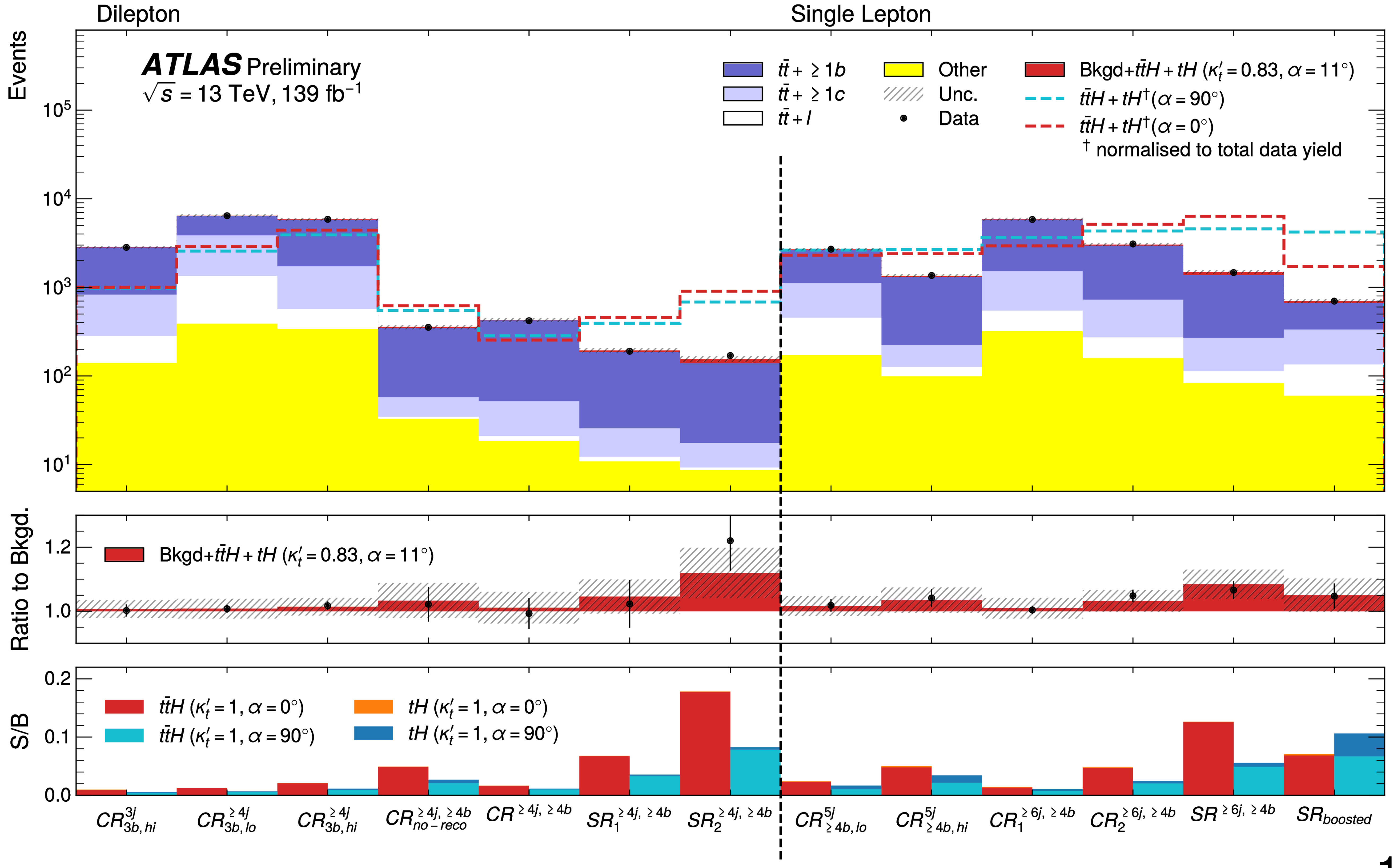

CP mixing angle measurement

τ-Higgs coupling in $\mathrm{H} \rightarrow \tau\tau$

ATLAS-CONF-2022-032

CP-sensitive observable: ϕ^{*}_{CP} (signed acoplanarity angle)

Different methods for tau lepton decay planes reconstruction

Signal events model w/o spin correlations -> introduced as per event weights

24 Signal Regions & 10 Control Regions in the fit

The precision is limited by the stat. uncertainties

τ lepton decay modes used in the analysis

Notation	Decay mode	Branching fraction
ℓ	$\ell^{\pm}\bar{\nu}\nu$	35.2 %
1p0n	$h^{\pm}\nu$ ($\pi^{\pm}\nu$)	11.5 % (10.8 %)
1p1n	$h^{\pm}\pi^{0}\nu$ ($\pi^{\pm}\pi^{0}\nu$)	25.9 % (25.5 %)
1pXn	$h^{\pm} \geq 2\pi^{0}\nu$ ($\pi^{\pm}2\pi^{0}\nu$)	10.8 % (9.3 %)
3p0n	$3h^{\pm}\nu$ ($3\pi^{\pm}\nu$)	9.8 % (9.0 %)

Impact of uncertainties

Set of nuisance parameters	Impact on ϕ_{τ} (°)
Jet	4.3
$E_{\mathrm{T}}^{\mathrm{miss}}$	0.4
Electron	0.3
Muon	0.9
τ_{had} reconstruction	1.0
Misidentified τ	0.6
τ_{had} decay mode classification	0.3
π^{0} angular resolution and energy scale	0.2
Track ($\pi^{\pm}$, impact parameter)	0.7
Flavour Tagging	0.2
Luminosity	0.1
Theory uncertainty in $H \rightarrow \tau\tau$ processes	1.5
Theory uncertainty in $Z \rightarrow \tau\tau$ processes	1.1
Simulated background sample statistics	1.4
Signal normalisation	1.4
Background normalisation	0.6
Total systematic uncertainty	5.2
Data sample statistics	15.6
Total	16.4

STXS

arXiv:2207.00348v1

$H \to \gamma\gamma$

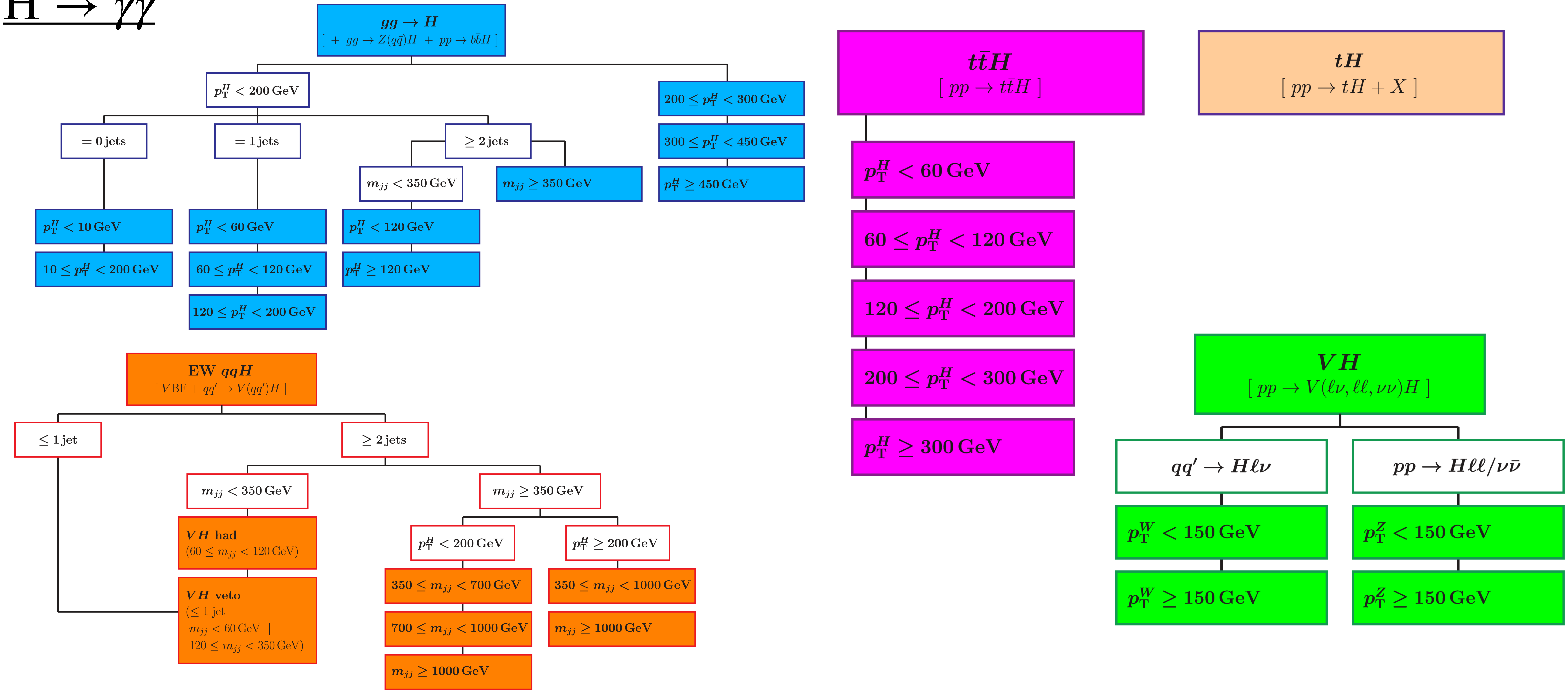

Correlation matrix

arXiv:2207.00348v1

$H \to \gamma\gamma$

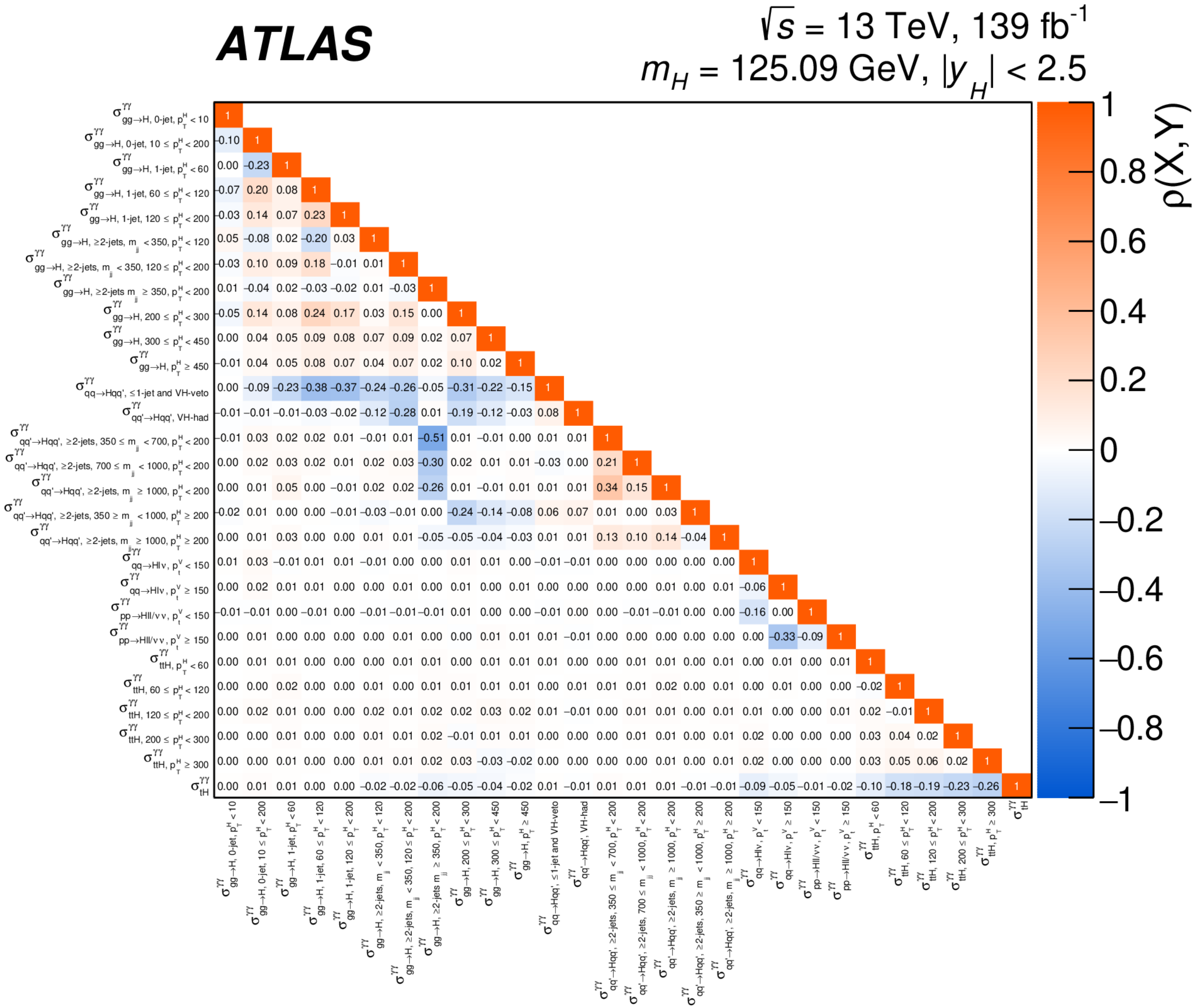

EFT interpretation

[arXiv:2207.00348v1](https://arxiv.org/abs/2207.00348v1)

$\mathrm{H} \rightarrow \gamma\gamma$

Coeff.	Operator	Incl.	Coeff.	Operator	Incl.
c_G	$f^{ABC} G_\mu^{A\nu} G_\nu^{B\rho} G_\rho^{C\mu}$	✓	$c_{qq}^{(3)}$	$(\bar{q}_r \gamma_\mu \tau^I q_r)(\bar{q}_s \gamma^\mu \tau^I q_s)$	✓
c_W	$\epsilon^{IJK} W_\mu^{I\nu} W_\nu^{J\rho} W_\rho^{K\mu}$	✓	$c_{qq}^{(3)\prime}$	$(\bar{q}_r \gamma_\mu \tau^I q_s)(\bar{q}_s \gamma^\mu \tau^I q_r)$	✓
c_H	$(H^\dagger H)^3$		$c_{qq}^{(1)}$	$(\bar{q}_r \gamma_\mu q_r)(\bar{q}_s \gamma^\mu q_s)$	✓
$c_{H\Box}$	$(H^\dagger H)\Box(H^\dagger H)$	✓	$c_{qq}^{(1)\prime}$	$(\bar{q}_r \gamma_\mu q_s)(\bar{q}_s \gamma^\mu q_r)$	✓
c_{HD}	$(H^\dagger D^\mu H)^* (H^\dagger D_\mu H)$	✓	$c_{lq}^{(3)}$	$(\bar{l}_r \gamma_\mu \tau^I l_r)(\bar{q}_s \gamma^\mu \tau^I q_s)$	
c_{HG}	$H^\dagger H\, G_{\mu\nu}^A G^{A\mu\nu}$	✓	$c_{lq}^{(1)}$	$(\bar{l}_r \gamma_\mu l_r)(\bar{q}_s \gamma^\mu q_s)$	
c_{HW}	$H^\dagger H\, W_{\mu\nu}^I W^{I\mu\nu}$	✓	c_{ee}	$(\bar{e}_r \gamma_\mu e_r)(\bar{e}_s \gamma^\mu e_s)$	
c_{HB}	$H^\dagger H\, B_{\mu\nu} B^{\mu\nu}$	✓	c_{eu}	$(\bar{e}_r \gamma_\mu e_r)(\bar{u}_s \gamma^\mu u_s)$	
c_{HWB}	$H^\dagger \tau^I H\, W_{\mu\nu}^I B^{\mu\nu}$	✓	c_{ed}	$(\bar{e}_r \gamma_\mu e_r)(\bar{d}_s \gamma^\mu d_s)$	
c_{eH}	$(H^\dagger H)(\bar{l}_p [Y_e^\dagger]_{pq} e_q H)$	✓	c_{uu}	$(\bar{u}_r \gamma_\mu u_r)(\bar{u}_s \gamma^\mu u_s)$	✓
c_{uH}	$(H^\dagger H)(\bar{q}_p [Y_u^\dagger]_{pq} u_q \widetilde{H})$	✓	c'_{uu}	$(\bar{u}_r \gamma_\mu u_s)(\bar{u}_s \gamma^\mu u_r)$	✓
c_{dH}	$(H^\dagger H)(\bar{q}_p [Y_d^\dagger]_{pq} d_q H)$	✓	c_{dd}	$(\bar{d}_r \gamma_\mu d_r)(\bar{d}_s \gamma^\mu d_s)$	
c_{eW}	$(\bar{l}_p \sigma^{\mu\nu} [Y_e^\dagger]_{pq} e_q) \tau^I H\, W_{\mu\nu}^I$		c'_{dd}	$(\bar{d}_r \gamma_\mu d_s)(\bar{d}_s \gamma^\mu d_r)$	
c_{eB}	$(\bar{l}_p \sigma^{\mu\nu} [Y_e^\dagger]_{pq} e_q) H\, B_{\mu\nu}$		$c_{ud}^{(1)}$	$(\bar{u}_r \gamma_\mu u_r)(\bar{d}_s \gamma^\mu d_s)$	✓
c_{uG}	$(\bar{q}_p \sigma^{\mu\nu} T^A [Y_u^\dagger]_{pq} u_q) \widetilde{H}\, G_{\mu\nu}^A$	✓	$c_{ud}^{(8)}$	$(\bar{u}_r \gamma_\mu T^A u_r)(\bar{d}_s \gamma^\mu T^A d_s)$	✓
c_{uW}	$(\bar{q}_p \sigma^{\mu\nu} [Y_u^\dagger]_{pq} u_q) \tau^I \widetilde{H}\, W_{\mu\nu}^I$	✓	c_{le}	$(\bar{l}_r \gamma_\mu l_r)(\bar{e}_s \gamma^\mu e_s)$	
c_{uB}	$(\bar{q}_p \sigma^{\mu\nu} [Y_u^\dagger]_{pq} u_q) \widetilde{H}\, B_{\mu\nu}$	✓	c_{lu}	$(\bar{l}_r \gamma_\mu l_r)(\bar{u}_s \gamma^\mu u_s)$	
c_{dG}	$(\bar{q}_p \sigma^{\mu\nu} T^A [Y_d^\dagger]_{pq} d_q) H\, G_{\mu\nu}^A$		c_{ld}	$(\bar{l}_r \gamma_\mu l_r)(\bar{d}_s \gamma^\mu d_s)$	
c_{dW}	$(\bar{q}_p \sigma^{\mu\nu} [Y_d^\dagger]_{pq} d_q) \tau^I H\, W_{\mu\nu}^I$		c_{qe}	$(\bar{q}_r \gamma_\mu q_r)(\bar{e}_s \gamma^\mu e_s)$	
c_{dB}	$(\bar{q}_p \sigma^{\mu\nu} [Y_d^\dagger]_{pq} d_q) H\, B_{\mu\nu}$		$c_{qu}^{(1)}$	$(\bar{q}_r \gamma_\mu q_r)(\bar{u}_s \gamma^\mu u_s)$	✓
$c_{Hl}^{(3)}$	$(H^\dagger i \overleftrightarrow{D}_\mu^I H)(\bar{l}_r \tau^I \gamma^\mu l_r)$	✓	$c_{qu}^{(8)}$	$(\bar{q}_r \gamma_\mu T^A q_r)(\bar{u}_s \gamma^\mu T^A u_s)$	✓
$c_{Hl}^{(1)}$	$(H^\dagger i \overleftrightarrow{D}_\mu H)(\bar{l}_r \gamma^\mu l_r)$	✓	$c_{qd}^{(1)}$	$(\bar{q}_r \gamma_\mu q_r)(\bar{d}_s \gamma^\mu d_s)$	✓
c_{He}	$(H^\dagger i \overleftrightarrow{D}_\mu H)(\bar{e}_r \gamma^\mu e_r)$	✓	$c_{qd}^{(8)}$	$(\bar{q}_r \gamma_\mu T^A q_r)(\bar{d}_s \gamma^\mu T^A d_s)$	✓

$c_{Hq}^{(3)}$	$(H^\dagger i \overleftrightarrow{D}_\mu^I H)(\bar{q}_r \tau^I \gamma^\mu q_r)$	✓	c_{ledq}	$(\bar{l}_p^j [Y_l^\dagger]_{pq} e_q)(\bar{d}_r [Y_d]_{rs} q_s^j)$	
$c_{Hq}^{(1)}$	$(H^\dagger i \overleftrightarrow{D}_\mu H)(\bar{q}_r \gamma^\mu q_r)$	✓	$c_{quqd}^{(1)}$	$(\bar{q}_p^j [Y_u^\dagger]_{pq} u_q) \epsilon_{jk} (\bar{q}_r^k [Y_d^\dagger]_{rs} d_s)$	
c_{Hu}	$(H^\dagger i \overleftrightarrow{D}_\mu H)(\bar{u}_r \gamma^\mu u_r)$	✓	$c_{quqd}^{(1)\prime}$	$(\bar{q}_p^j [Y_d^\dagger]_{ps} u_q) \epsilon_{jk} (\bar{q}_r^k [Y_u^\dagger]_{rq} d_s)$	
c_{Hd}	$(H^\dagger i \overleftrightarrow{D}_\mu H)(\bar{d}_r \gamma^\mu d_r)$	✓	$c_{quqd}^{(8)}$	$(\bar{q}_p^j T^A [Y_u^\dagger]_{pq} u_q) \epsilon_{jk} (\bar{q}_r^k T^A [Y_d^\dagger]_{rs} d_s)$	
c_{Hud}	$(H^\dagger i D_\mu H)(\bar{u}_p \gamma^\mu [Y_u Y_d^\dagger]_{pq} d_q)$		$c_{quqd}^{(8)\prime}$	$(\bar{q}_p^j T^A [Y_d^\dagger]_{ps} u_q) \epsilon_{jk} (\bar{q}_r^k T^A [Y_u^\dagger]_{rq} d_s)$	
c_{ll}	$(\bar{l}_r \gamma_\mu l_r)(\bar{l}_s \gamma^\mu l_s)$		$c_{lequ}^{(1)}$	$(\bar{l}_p^j [Y_e^\dagger]_{pq} e_q) \epsilon_{jk} (\bar{q}_r^k [Y_u^\dagger]_{rs} u_s)$	
c'_{ll}	$(\bar{l}_r \gamma_\mu l_s)(\bar{l}_s \gamma^\mu l_r)$	✓	$c_{lequ}^{(3)}$	$(\bar{l}_p^j \sigma^{\mu\nu} [Y_e^\dagger]_{ps} e_q) \epsilon_{jk} (\bar{q}_r^k \sigma_{\mu\nu} [Y_u^\dagger]_{rq} u_s)$	

Differential cross sections measurements

arXiv:2207.08615v1

$H \rightarrow \gamma\gamma$ and $H \rightarrow ZZ^* \rightarrow 4\ell$

Acceptance factors

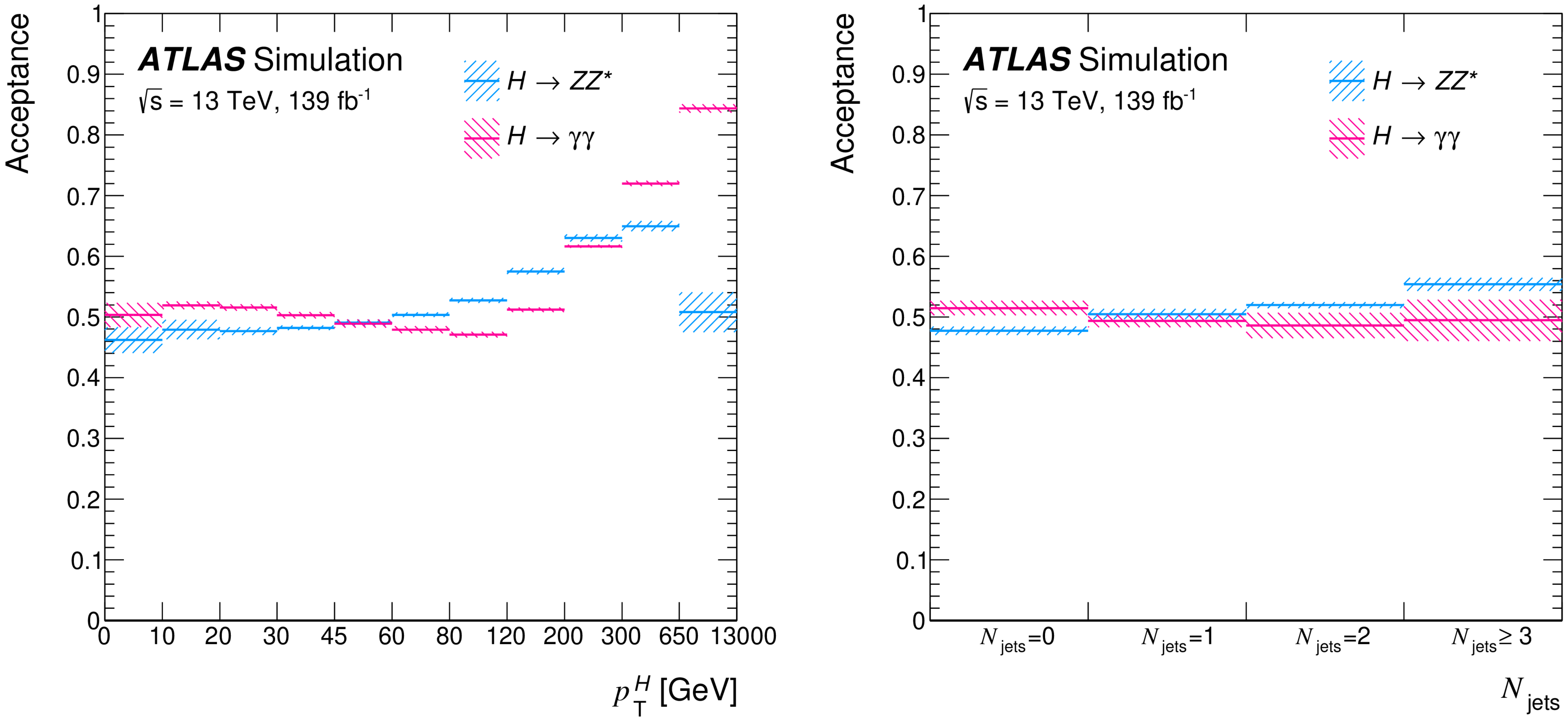

Fiducial phase space

p_T^H and $|y_H|$ derived from decay products

Total phase space

p_T^H and $|y_H|$ derived from simulation

Acceptance factors ~ 50%

Combination analysis inputs

arXiv:2207.00348v1

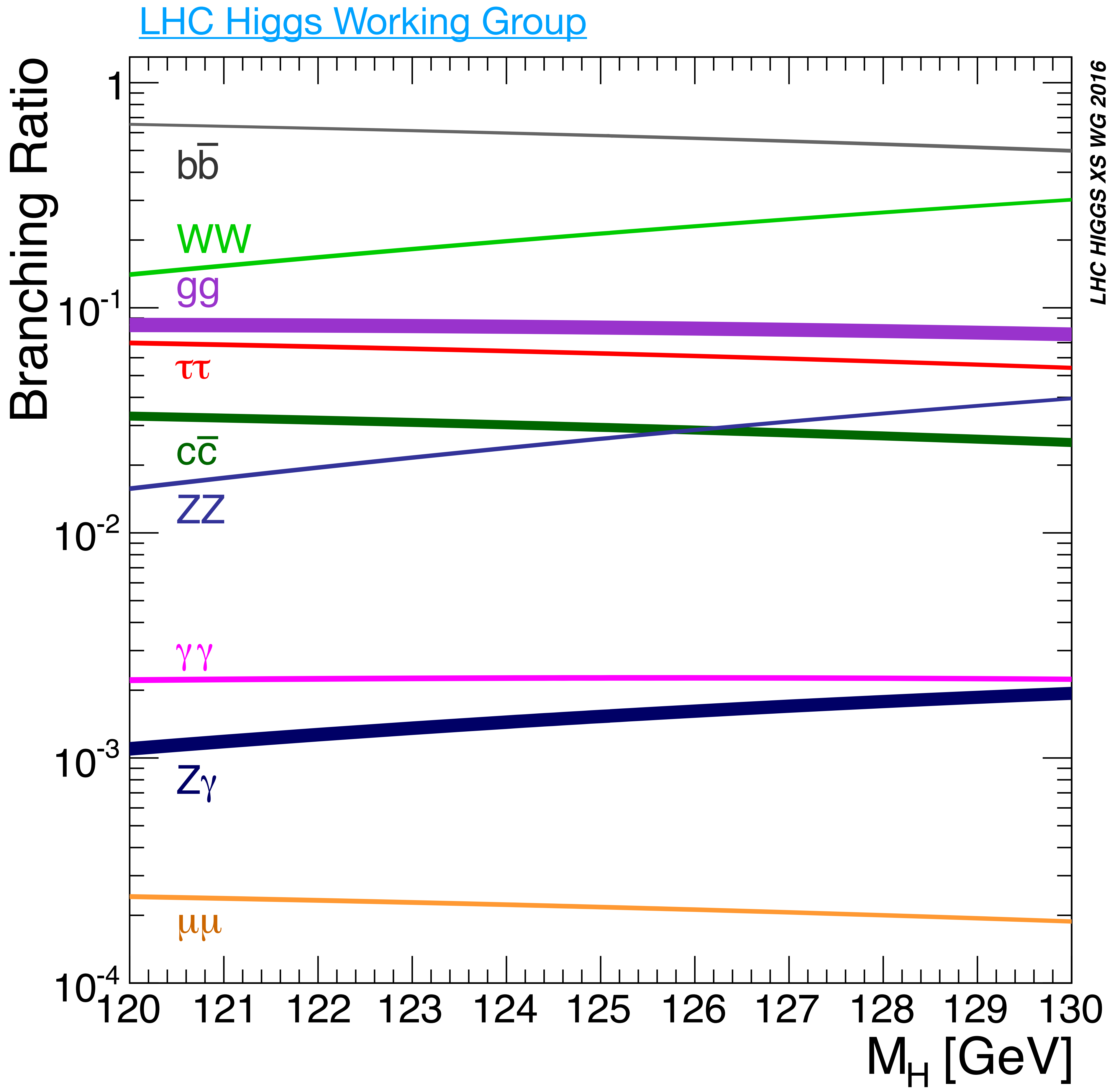

Decay mode	Targeted production processes	$\mathcal{L}$ [fb^{-1}]	Ref.	Fits deployed in
$H \to \gamma\gamma$	ggF, VBF, $WH, ZH, t\bar{t}H, tH$	139	[31]	All
$H \to ZZ$	ggF, VBF, $WH + ZH, t\bar{t}H + tH$	139	[28]	All
	$t\bar{t}H + tH$ (multilepton)	36.1	[39]	All but fit of kinematics
$H \to WW$	ggF, VBF	139	[29]	All
	WH, ZH	36.1	[30]	All but fit of kinematics
	$t\bar{t}H + tH$ (multilepton)	36.1	[39]	All but fit of kinematics
$H \to Z\gamma$	inclusive	139	[32]	All but fit of kinematics
$H \to b\bar{b}$	WH, ZH	139	[33, 34]	All
	VBF	126	[35]	All
	$t\bar{t}H + tH$	139	[36]	All
	inclusive	139	[37]	Only for fit of kinematics
$H \to \tau\tau$	ggF, VBF, $WH + ZH, t\bar{t}H + tH$	139	[38]	All
	$t\bar{t}H + tH$ (multilepton)	36.1	[39]	All but fit of kinematics
$H \to \mu\mu$	ggF + $t\bar{t}H + tH$, VBF + $WH + ZH$	139	[40]	All but fit of kinematics
$H \to c\bar{c}$	$WH + ZH$	139	[41]	Only for free-floating κ_c
$H \to$ invisible	VBF	139	[42]	κ models with $B_{u.}$ & $B_{inv.}$
	ZH	139	[43]	κ models with $B_{u.}$ & $B_{inv.}$